https://doi.org/10.5194/acp-2020-665
Preprint. Discussion started: 28 July 2020

Atmospheric Chemistry and Physics Discussions

The importance of Aitken mode aerosol particles for cloud sustenance in the summertime high Arctic: A simulation study supported by observational data

Ines Bulatovic[1,2], Adele L. Igel[3], Caroline Leck[1,2], Jost Heintzenberg[1,5], Ilona Riipinen[4,2] and Annica M. L. Ekman[1,2]

[1]Department of Meteorology, Stockholm University, Stockholm, 106 91, Sweden
[2]Bolin Centre for Climate Change, Stockholm, 106 91, Sweden
[3]Department of Land, Air and Water Resources, University of California, Davis, Davis, CA 95616, California
[4]Department of Environmental Science (ACES), Stockholm University, Stockholm, 106 91, Sweden
[5]Leibniz Institute for Tropospheric Research, Permoserstr. 14, Leipzig, 04318, Germany

Correspondence to: Ines Bulatovic (ines.bulatovic@misu.su.se)

Abstract. The potential importance of Aitken mode particles (diameters ~25–80 nm) for stratiform mixed-phase clouds in the summertime high Arctic has been investigated using two large-eddy simulation models. We find that in both models Aitken mode particles significantly affect the simulated cloud properties and can help sustain the cloud when accumulation mode concentrations are low (<10–20 cm^{-3}), even when the particles have low hygroscopicity (hygroscopicity parameter κ=0.1). However, the influence of the Aitken mode decreases if the overall liquid water content of the cloud is low, either due to a higher ice fraction or due to low radiative cooling rates. An analysis of the simulated supersaturation (ss) statistics shows that the ss frequently reaches 0.5% and sometimes even exceeds 1%, which confirms that Aitken mode particles can be activated. The modelling results are in qualitative agreement with observations of the Hoppel minimum obtained from four different expeditions in the high Arctic. Our findings highlight the importance of better understanding Aitken mode particle formation, chemical properties and emissions, in particular in clean environments such as the high Arctic.

1 Introduction

The Arctic region is experiencing a rapid increase in surface temperature that is substantially larger than the global average increase (Holland and Bitz, 2003; Hartmann et al., 2013). The enhanced Arctic warming, known as the Arctic amplification, is a result of remote forcings (which modify heat and moisture transport from lower latitudes) as well as local drivers and feedbacks (e.g., local aerosol sources, cloud and ice-albedo feedbacks; Serreze and Barry, 2011; Stjern et al., 2019). Changes in the dynamical and microphysical properties of clouds are central to local feedbacks (Curry et al., 1996; Garrett et al., 2009; Kay et al., 2011) due to the strong impact of clouds on the surface energy budget (Curry and Ebert, 1992; Shupe and Intrieri, 2004) and subsequent sea-ice growth (Kay and Gettelman, 2009; Kay et al., 2011; Tjernström et al., 2015).

In the high Arctic (north of 80° N), stratiform mixed-phase (SMP) clouds are permanent and ubiquitous (Shupe et al., 2006; Shupe et al., 2013). Despite the presence of liquid and ice in the same volume and a continuous sink of the liquid phase through ice growth and precipitation, these clouds may persist for several days (Shupe et al., 2006). A layer of liquid is typically present at the top of SMP clouds. Maintenance of this layer is critical for sustaining longwave emission and ensuing cooling at the cloud top (e.g., Persson et al, 2017; Dimitrelos et al., 2020), which enhances a buoyancy-driven turbulent mixing in a layer below associated with the cloud (Tjernström et al., 2005). The turbulence further influences cloud liquid growth. Strong overturning means strong updrafts that allow efficient condensation of vapor onto cloud droplets. It also leads to higher entrainment rates at the cloud top (Tjernström, 2007). A peculiar feature of the high Arctic is that the specific humidity frequently increases over the inversion layer that caps the low-level SMP clouds (Sedlar et al., 2012; Shupe et al., 2013). Entrainment may thus bring more vapor into the cloud and moisten the boundary layer (Tjernström et al., 2012; Shupe et al., 2013). This and other conditions specific for boundary layers in the high Arctic allow liquid water to persist, and thereby also prevent quick cloud glaciation, despite an opposing effect of ice growth within the cloud (e.g., Morrison et al., 2012). In contrast to low-level clouds at lower latitudes, SMP clouds in the high Arctic have a net positive effect on the surface energy budget during most of the year. Due to a low amount of solar radiation in this region, the warming induced by cloud longwave emission towards the surface is generally larger than the cooling effect due to reflection of solar radiation. However, during the peak-melt season at the end of the summer, SMP clouds can

https://doi.org/10.5194/acp-2020-665
Preprint. Discussion started: 28 July 2020

Atmospheric Chemistry and Physics Discussions

have a net cooling effect on the surface energy budget and thereby influence the timing of the autumn freeze-up (e.g., Intrieri et al., 2002; Shupe and Intrieri, 2004; Tjernström et al., 2014).

Aerosol particles can act as cloud condensation nuclei (CCN) and ice nucleating particles (INP), which affect the microphysical and optical properties of clouds (referred to as aerosol indirect effects). Clouds in the Arctic, especially those over the pack ice in the summertime, appear to be particularly sensitive to perturbations in the aerosol population due to the generally pristine conditions (Bigg and Leck, 2001). Droplet number concentrations are often low (Leck and Svensson, 2015), and thus even small changes in the availability of CCN may have a critical impact on the radiative fluxes and surface energy balance (Garrett et al., 2002; Lubin and Vogelmann, 2006; Mauritsen et al., 2011). Therefore, there is a need to better understand sources and sinks of high Arctic aerosols as well as their chemical composition, physical characteristics and potential effects on cloud formation. However, due to the harsh conditions, measurements are sparse and generally limited to summertime. When long-range transport of aerosols over the pack ice is small, as in summer, the surface number concentrations of accumulation mode particles (sizes typically 80–500 nm; Covert et al., 1996) are generally below 100 cm^{-3} and occasionally below 1 cm^{-3} (Bigg et al., 1996; Mauritsen et al., 2011; Heintzenberg et al., 2015; Leck and Svensson, 2015). During this time of the year, marine biological activity could provide a source of small, airborne particles, adding to the mass and number of the Aitken mode particles (sizes typically 25–80 nm; Covert et al., 1996) (Leck and Bigg, 2005a; Heintzenberg and Leck, 2012; Karl et al., 2013; Heintzenberg et al., 2015).

The ability of an aerosol particle to act as a CCN depends upon multiple factors, such as its size and chemical composition (Köhler, 1936), surface tension (e.g., Lowe et al., 2019) and the ambient relative humidity (e.g., Rastak et al., 2017). A larger maximum supersaturation within an air parcel allows smaller and less hygroscopic particles potentially to act as CCN (Köhler, 1936; Petters and Kreidenweis, 2007). On the other hand, the maximum supersaturation is also dependent on the relative abundance of particles, in particular the number of water soluble accumulation or coarse mode particles as they easily act as CCN and subsequently take up water when they grow (e.g., Ghan et al., 1997). Therefore, typical CCN sizes differ among the environments with different aerosol size distributions, compositions and supersaturation values (Seinfeld and Pandis, 2006). In general, water soluble particles within the accumulation mode constitute the largest source of atmospheric CCN (Seinfeld and Pandis, 2006). However, in the summertime Arctic, a relatively low condensation sink of water vapor due to the low number of accumulation mode particles may lead to relatively large maximum supersaturations that could allow Aitken mode particles to act as CCN. Recent observations for the Arctic region south of the ice edge, which focus or include summertime season, have indeed suggested that particles with diameters below 50 nm can be CCN-active (Willis et al., 2016; Kecorius et al., 2019; Koike at al., 2019). However, these studies were not focused on the high Arctic and they only indirectly inferred the potential importance of Aitken mode particles as CCN. The situation over the pack ice is unique and the knowledge that we have from other regions south of the ice edge may not be directly applicable. Model simulations by Christiansen et al. (2020) have indicated that Aitken mode particles can influence high Arctic cloud properties, but these simulations only consider extreme conditions with no accumulation mode aerosols present in the atmosphere.

Summarizing, we know that high Arctic summertime SMP clouds over the pack ice are governed by a complex interplay between dynamics, cloud microphysics and aerosols and that they strongly influence climate, however, there are still many uncertainties regarding these clouds. One knowledge gap is if and under which conditions Aitken mode particles become CCN-active in this environment and how these particles then may affect the microphysical properties of the clouds. In this study, we therefore employ two different large-eddy simulation (LES) models to simulate a relatively long-lived summertime cloud observed in the high Arctic during the ASCOS campaign (Tjernström et al., 2014). During the campaign, measurements often showed low concentrations of accumulation mode particles while the concentration of Aitken mode particles was relatively high (Leck and Svensson, 2015). We initialize the models with a range of aerosol size distributions and explore if Aitken mode particles can help sustain the cloud, or if accumulation mode aerosols dominate the control of cloud properties (i.e. cloud droplet, rain and ice mixing ratios) even at low total aerosol concentrations. We also analyze the maximum supersaturations simulated by the two models and calculate the corresponding threshold diameters of aerosol activation. The engagement of two different models allows us to evaluate if the results are dependent on the details of a specific model or if we can draw more general conclusions. Finally, we introduce the statistics of the aerosol size distributions (Heintzenberg and Leck, 2012) observed during the summers of four different high Arctic campaigns that took place in 1991, 1996, 2001 and 2008 year (Leck et al., 1996; Leck et al., 2001; Leck et al., 2004; Tjernstöm et al., 2014) and compare them with the simulated results. The general conclusions are provided at the end of the study.

https://doi.org/10.5194/acp-2020-665
Preprint. Discussion started: 28 July 2020

Atmospheric Chemistry and Physics Discussions

2 Method

2.1 Models

The simulations were performed using two models. MIMICA (the MISU MIT Cloud-Aerosol Model) is an LES model and solves the equations for a non-hydrostatic, anelastic atmospheric system (Savre et al., 2014). The model uses a two-moment bulk microphysics scheme (Seifert and Beheng, 2001) to calculate the prognostic variables (i.e. mass mixing ratio and number concentration) of five different hydrometeor types considered, namely cloud droplets, raindrops, cloud ice, graupel and snow. All hydrometeor categories have mass distributions in the form of regular gamma functions. Autoconversion and self-collection of liquid particles are also calculated as described in Seifert and Beheng (2001). A pseudo-analytic method is used to model the supersaturation, with the integration of condensation/evaporation at the model time step of ~2 s (Morrison and Grabowski, 2008). The terminal fall speed of the hydrometeors is calculated using a simple power law of the diameter of the particle, which determines the wet deposition. To represent an aerosol population of different particle sizes and chemical compositions, MIMICA includes a two-moment aerosol module (Ekman et al., 2006). All aerosol modes are described with lognormal distributions. In the model, aerosols can act as cloud condensation nuclei following kappa-Köhler theory (Petters and Kreidenweis, 2007), but not as ice nuclei. The number concentration of ice crystals is prescribed to 0.2 L^{-1} and it is kept quasi-constant during the simulations (Ovchinnikov et al., 2011, 2014). This parameterization mimics immersion freezing, i.e. ice can only form if there is supercooled water present. Secondary ice production and aggregation of ice crystals are omitted in MIMICA. The radiative transfer is calculated following a four-stream radiative transfer solver (Fu and Liou, 1993), which includes 6 bands for shortwave and 12 bands for longwave radiation. The model domain is three-dimensional and it is defined by 96 × 96 × 128 grid-points. In the horizontal direction, there is a fixed grid distance between the grids of 62.5 m. In the vertical direction, the grid is variable with the highest resolution (7.5 m) at the surface and in the cloud layer.

The second model used is the Regional Atmospheric Modeling System (RAMS; Cotton et al., 2003). RAMS is a flexible model that is most commonly used for cloud-resolving and large eddy simulations. It uses a two-moment bin-emulating bulk microphysics scheme to predict the mass and number mixing ratios of liquid and ice hydrometeor species (Meyers et al., 1997; Saleeby and van den Heever, 2013). In this study, six species are used, namely, cloud droplets, raindrops, cloud ice, snow, graupel and hail. RAMS typically uses two cloud ice species, but only one was used in this study with a prescribed concentration of 0.2 L^{-1} as was done in MIMICA. Collision-coalescence of liquid drops is done through the use of lookup tables that are generated by solving the stochastic collection equation (Feingold et al., 1997). Condensation depends explicitly on the hydrometeor properties and allows for supersaturation at the end of the time step (Walko et al., 2000). RAMS also includes a user-defined number of lognormal aerosol distributions. Aerosol particles act as CCN and are activated using additional look-up tables generated from an offline parcel model based on kappa-Köhler theory (Saleeby and van den Heever, 2013). Unlike MIMICA, aggregation of ice crystals is permitted. Radiative transfer is calculated following Harrington (1997). The model domain uses the same horizontal specification as MIMICA, but vertical grid spacing is kept constant at 10 m.

2.2 Overview of the simulated case: The ASCOS campaign

The Arctic Summer Cloud Ocean Study (ASCOS) campaign took place in the summer of 2008 onboard the Swedish icebreaker *Oden*, including a three-week ice drift with enhanced meteorology measurements when *Oden* was anchored to a large ice floe slightly north of 87° N. A full description of the expedition can be found in Tjernström et al. (2014). This campaign has so far been one of the most extensive studies in the central Arctic focusing on the atmosphere, clouds and aerosol properties and their linkages to the microbiological life in the upper ocean. To investigate a case with a quasi-steady-state cloud regime, the simulations are based on a period that was characterized by a persistent, low-level SMP cloud observed from 18 UTC 30 August to 12 UTC 31 August 2008. The period represents one of the last days of the ice drift episode, which took place from 12 August to 2 September 2008. During this period, the number concentration of accumulation mode particles was relatively low (Leck and Svensson, 2015). Therefore, a change in the aerosol population could be particularly important for inducing cloud perturbations that may affect the surface energy budget.

Radiosondes were launched every 6 h and provided profiles of thermodynamic properties (e.g., pressure, temperature, relative humidity) and wind speeds. The one from approximately 06 UTC 31 August 2008 was representative of the conditions observed during the whole stratocumulus period and used to initialize the simulations. Cloud properties and thermodynamic characteristics of the atmosphere were monitored with surface-based remote sensing instruments (Shupe et al., 2013). The cloud base and cloud top were nearly constant during the cloud lifetime (500 and 1000 m, respectively). Retrievals of liquid water path (LWP) were made from the 23 and 30 GHz microwave radiometer measurements (Sedlar and Shupe, 2014). The observed LWP uncertainty was around ~25 g m^{-2} while the uncertainty in the ice water path (IWP) was about a factor of 2 (Shupe et al., 2008;

https://doi.org/10.5194/acp-2020-665
Preprint. Discussion started: 28 July 2020

Atmospheric Chemistry and Physics Discussions

Birch et al., 2012). A CCN counter that was situated on *Oden*, at 25 m above the sea surface, measured a mean CCN concentration of about 25 cm^{-3} at a supersaturation of 0.2 % during the period of the ice drift (Martin et al., 2011; Leck and Svensson, 2015). The ship and the inlets were facing the wind so that local pollution from the ship was avoided. Additionally, a pollution controller was used to prevent direct contamination from the ship and the main pumps were turned off whenever the conditions for a clean environment were not completely satisfied (details on the pollution control system can be found in Leck et al., 2001 and in Tjernström et al., 2014).

2.3 Simulation setup

To investigate the influence of Aitken mode particles on cloud properties, and how this influence depends on the background concentration of accumulation mode aerosols, we have performed simulations with different prescribed aerosol size distributions. This means that there is no sink or source of aerosols within the model domain during the whole simulations for both models. We conduct two sets of simulations with two different background concentrations of the Aitken mode particles (20 and 200 cm^{-3}). Each set contains five cases with different levels of accumulation mode particles (0, 3, 5, 10 and 20 cm^{-3}), i.e. 10 simulations in total. All particle concentrations are assumed to be constant with height. The simulations are named by a combination of two numbers, where the first number refers to the accumulation mode and the second to the Aitken mode number concentration (e.g., the case with 0 cm^{-3} of accumulation and 20 cm^{-3} of Aitken mode particles is referred to as the AC0_AK20 simulation). The concentrations are chosen to cover typical aerosol size distributions often encountered in the summertime high Arctic (Heintzenberg and Leck, 2012; Leck and Svensson, 2015). If it is considered that the accumulation mode contributes most to atmospheric CCN, then the simulation with 20 cm^{-3} of both accumulation and Aitken mode aerosols agrees the best with the observations in terms of the CCN concentrations measured onboard the ship (Sect. 2.2). In this study, the simulation AC20_AK20 is thus considered as the baseline simulation.

A full description of meteorological conditions during the ASCOS campaign is available in Tjernström et al. (2012). The values used for the surface temperature and surface pressure are 269.8 K and 1026.3 hPa, respectively. The surface albedo is set to 0.844. The observed turbulent fluxes were small thus the sensible and latent heat fluxes are prescribed to zero. Over the whole model domain, the large-scale divergence is set to 1.5 x 10^{-6} s^{-1} in both models. The aerosol population in both modes is represented by lognormal functions with the distribution parameters based on the ASCOS campaign measurements (Igel et al., 2017). Modal diameters of 32 and 93 nm and standard deviations and 1.1 and 1.5 are used for the Aitken and accumulation modes, respectively. The simulations are initialized with prescribed cloud water mixing ratios derived from the observations, i.e. a cloud is present at the beginning of all simulations. The 3D model domain covers a region of 6 × 6 × 1.7 km^3. The simulation period is 12 hours, where the first 2 h are considered as a spin-up period and they are therefore excluded from the figures and analyses.

In clean environments, the source of Aitken mode aerosols is typically new particle formation (NPF) and subsequent growth. In the high Arctic, however, different sources of Aitken mode aerosols have been proposed. Some studies associate the Aitken mode with the NPF events and subsequent growth by DMS oxidation products (Wiedensohler et al., 1996). Other studies suggest that the Aitken mode particles in this region are made up of marine gels produced by phytoplankton and sea-ice algae at the sea-surface interface (Leck and Bigg, 2005b). Different mechanisms imply different chemical compositions and thereby different hygroscopic properties that aerosol particles might have in the high Arctic. To study the impact of aerosol hygroscopicity, we have performed additional simulations with different values of the hygroscopicity parameter, kappa, κ (Petters and Kreidenweis, 2007). The default κ-value used to describe the hygroscopic properties of both aerosol modes is set to 0.4 (Leck and Svensson, 2015). As some previous studies (e.g., Christiansen et al., 2020) have shown that a change in hygroscopicity of the accumulation mode aerosols has almost no influence on the cloud properties, we have only examined the sensitivity of the κ-value of the Aitken mode particles. Simulations AC3_AK20 and AC3_AK200 have been performed with two additional κ-values = [0.1, 1.1], which cover a typical range of hygroscopicity of compounds expected to be present in high Arctic Aitken mode particles (Leck and Svensson, 2015). The lower limit of the hygroscopicity parameter tested (κ=0.1) would be representative of e.g., many organic compounds (e.g., Leck and Svensson, 2015) while the upper limit prescribed (κ=1.1) would correspond to a water-soluble inorganic salt like ammonium sulfate (Petters and Kreidenweis, 2007).

We have also used MIMICA to examine how the influence of Aitken mode particles on cloud microphysical properties depends on the amount of ice present in the cloud. Additional versions of the simulations AC3_AK20 and AC3_AK200 have been performed with prescribed values of the ice crystal concentrations set to 0 and 1 L^{-1}. These values were chosen somewhat arbitrarily but should represent a range describing a relatively ice-free and an ice-rich cloud in the high Arctic.

https://doi.org/10.5194/acp-2020-665
Preprint. Discussion started: 28 July 2020

Atmospheric Chemistry and Physics Discussions

3 Simulation results

3.1 Baseline simulation: comparison of simulated cloud properties

We first compare our baseline simulations (AC20_AK20) with time series of observed LWP and IWP (Fig. 1).

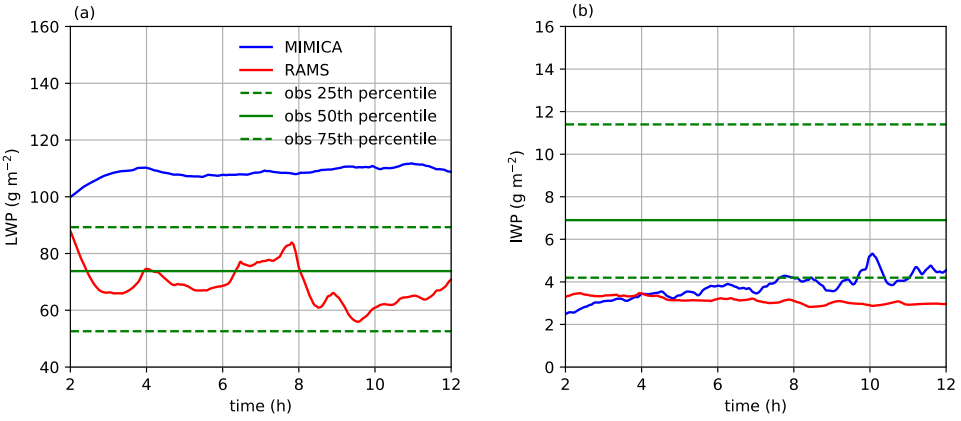

Figure 1: (a) LWP and (b) IWP simulated by MIMICA and RAMS for the baseline simulations, i.e. with accumulation and Aitken mode concentrations of 20 cm^{-3}. The retrieved values of LWP and IWP for the observed period are shown as 25th, 50th (median) and 75th percentiles. The first 2 h of simulations are excluded as they are considered as a spin-up period.

RAMS produces LWP values that fall within the observed range whereas MIMICA simulates a LWP that is 12–25 % higher than the 75th percentile of the observed range (Fig. 1a). In general, the use of prescribed aerosol particle concentrations should result in a higher LWP than if the simulations were performed with interactive aerosol particle concentrations (e.g., Stevens et al., 2018). It may be that MIMICA is more sensitive than RAMS in this regard. Furthermore, RAMS simulates weaker radiative cooling rates than MIMICA, which should produce a lower LWP in RAMS compared to MIMICA (see Sect. 3.2). Another possible reason for the discrepancy in the simulated LWP between the two models could be the different vertical resolutions in MIMICA and RAMS, which in MIMICA is higher in the cloud layer (Sect. 2.1). The simulated IWP in both models is close to the 25th percentile of the observed range (Fig. 1b). In MIMICA, the IWP overlaps with the 25th percentile value in the second half of the simulation while in RAMS it is 17–33 % lower than it. Overall, the results show that both models simulate reasonable LWP and IWP compared to the observational data, however, it is hard to conclude which model is better due to the large uncertainty and variability of the retrieved cloud variables (cf. Sect. 2.2).

Simulated cloud droplet, rain and total ice mixing ratios for the baseline simulation are shown for the two models in Fig. 2. The cloud droplet mixing ratio increases towards the top of the cloud in both models, but MIMICA produces slightly higher values in the upper part of the cloud layer (Fig. 2a and 2b) as was also reflected in the LWP values (Fig. 1a). There is also a difference in the cloud top height evolution, which in MIMICA increases with time whereas it remains constant in RAMS. Fig. 2c and 2d display that RAMS produces slightly more rain below the cloud than MIMICA. Both models simulate similar values of total ice, although MIMICA produces a few stronger vertical bands after 6 h of simulation (Fig. 2e and 2f). To better understand the cloud dynamics, we have also examined the cloud diagnostics (i.e. mass transfer rates between gas and condensed phases) for cloud droplet water, rainwater and ice crystals (Fig. 3). In MIMICA, cloud droplet water has the highest condensation rates at the top of the cloud whereas in RAMS they are homogenously distributed within the cloud layer (Fig. 3a and 3b). The reason is most likely the higher entrainment rates at cloud top in MIMICA (not shown) that bring more water vapor into the cloud from the moist air that is usually present above the stratocumulus-topped boundary layers in the high Arctic (Sedlar et al., 2012; Shupe et al., 2013). Higher entrainment rates are also consistent with the higher cloud top cooling rates present in MIMICA. Below cloud base, there is first a thin layer of cloud droplet evaporation present in both models, below which is a sub-cloud condensation layer in RAMS. This condensation layer is produced by weak sub-cloud convection (not shown). Even though the condensation is infrequent, the associated mean rates are of the same order of magnitude as the condensation rates within the main cloud layer. The pockets of condensation and evaporation present in the main cloud layer are well-correlated with updrafts and downdrafts and they tend to cancel each other in the mean. This is why the average condensation rate in the main cloud is of the same order of magnitude as the one in the sub-cloud layer. However, if we consider the domain

https://doi.org/10.5194/acp-2020-665
Preprint. Discussion started: 28 July 2020

Atmospheric Chemistry and Physics Discussions

median instead of the mean, then the condensation rates are higher within the main cloud layer and they are zero below the evaporation layer in RAMS (not shown). In both models, the condensational growth of raindrops is limited to the upper part of the cloud layer, while the maximum evaporation rates are found around the cloud base (Fig. 3c and 3d). This typically happens when the environment is subsaturated for liquid water but supersaturated for ice, which results in evaporation of raindrops and the growth of ice crystals. Ice crystals grow throughout the whole cloud layer with the highest deposition rates around cloud base (Fig. 3e and 3f), which corresponds well to the highest rain evaporation rates that are clearly seen in the MIMICA results (Fig. 3c). The ice crystal deposition and sublimation rates are higher in RAMS than in MIMICA since the two models partition the total ice deposition differently among ice hydrometeor categories. Examining the total ice deposition/sublimation rates would most likely lead to similar rates between the two models, but these rates are not available in MIMICA. The comparison shows that the simulated cloud microphysical properties are all within the same order of magnitude for the two models, i.e. both models in general simulate the same cloud mechanisms leading to cloud dynamics that are similar in many aspects. However, there are still some notable differences that arise from the different model descriptions.

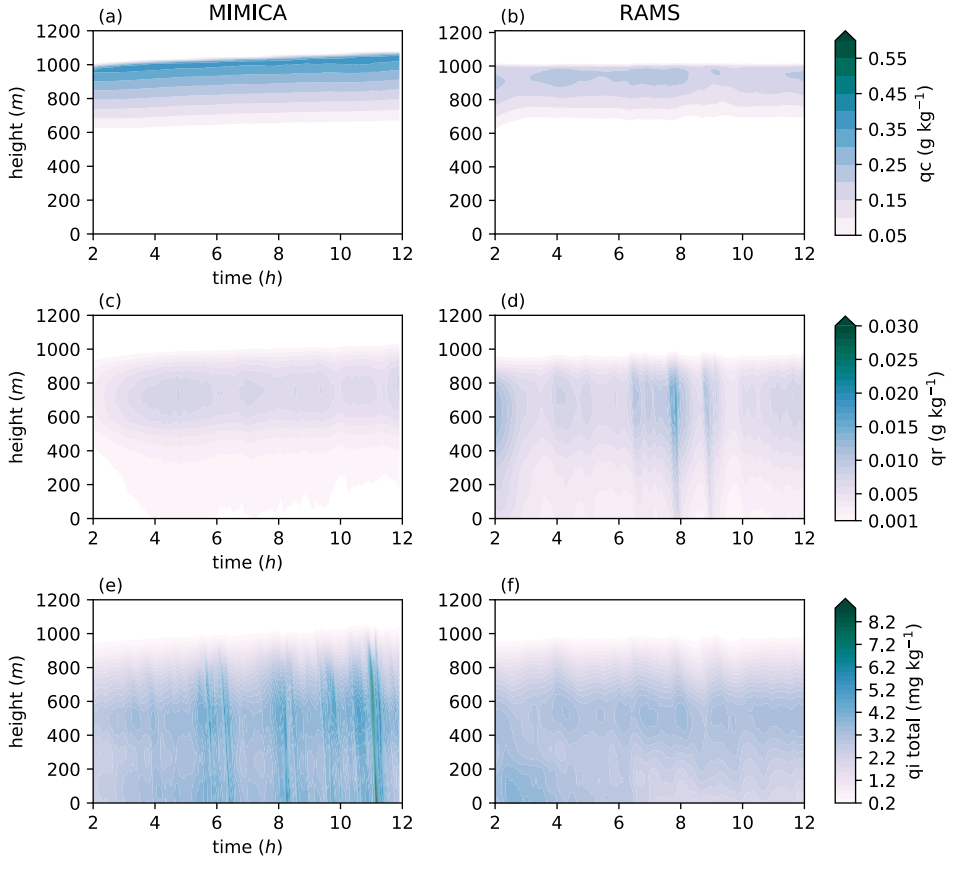

Figure 2: Cloud properties simulated by MIMICA and RAMS for the baseline simulation, i.e. with accumulation and Aitken mode concentrations of 20 cm^{-3}. (a,b) cloud droplet mixing ratio (qc); (c,d) rain mixing ratio (qr); (e,f) total ice (ice crystals, graupel (and hail for RAMS)) mixing ratio (qi total). The first 2 h of simulations are excluded as they are considered as a spin-up period.

https://doi.org/10.5194/acp-2020-665
Preprint. Discussion started: 28 July 2020

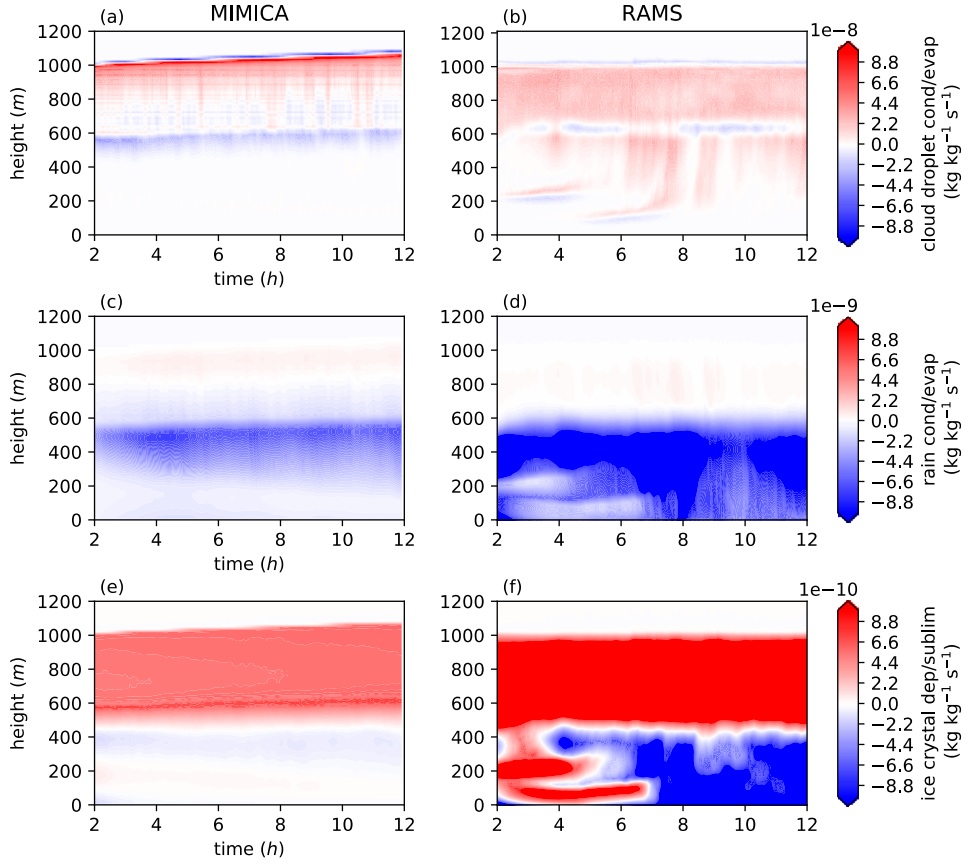

Figure 3: Cloud diagnostics simulated by MIMICA and RAMS for the baseline simulation, i.e. with accumulation and Aitken mode concentrations of 20 cm-3. (a,b) cloud droplet condensation/evaporation rates; (c,d) rain drop condensation/evaporation rates; (e,f) ice crystal deposition/sublimation rates. The first 2 h of simulations are excluded as they are considered as a spin-up period. Red color indicates net condensation/deposition and blue net evaporation/sublimation.

https://doi.org/10.5194/acp-2020-665
Preprint. Discussion started: 28 July 2020

Atmospheric Chemistry and Physics Discussions

3.2 Processes maintaining the simulated high Arctic SMP cloud

The cloud droplet mixing ratio for all simulations is shown in Fig. 4. In general, MIMICA simulates a thicker cloud than RAMS. In both models, the cloud shrinks at the beginning of the simulation (especially pronounced in the cases with low accumulation mode particle concentrations). However, the turbulence in MIMICA is strong enough to develop and maintain a stable cloud with time for all cases while this is not true for RAMS, where the cloud dissipates completely in the simulations with 0 cm^{-3} of accumulation mode particles (i.e. AC0_AK20 and AC0_AK200 simulations). As one of the main generators of cloud turbulence is radiative cooling at the top of the cloud, we have compared the cooling rates between the two models. The cloud top cooling rates in MIMICA are about two to three times greater than those in RAMS (Fig. 5 and A2) and more similar to values obtained from radiative transfer calculations based on observational data (Brooks et al., 2017). Most of the difference between the cooling rates is due to the cloud top liquid water content being about twice as large in MIMICA (Fig. 4). However, the cooling rates in RAMS are smaller even at the beginning of the simulation when the liquid water contents are very similar in the two models, so the difference in liquid water content (Fig. 1a) cannot be the only explanation. A less efficient radiative cooling parameterization in RAMS could explain the discrepancy in simulated cloud droplet mixing ratios since lower radiative cooling at the top of the cloud leads to less turbulence in the cloud layer and consequently to less cloud water (as the free troposphere in the simulated case is a source of moisture to the cloud layer, cf. Sect. 1). To further investigate how the radiation parametrization can influence the model results, we have performed additional simulations with MIMICA and RAMS where the models were utilized with simplified radiative transfer schemes or with a prescribed higher cooling rate at the cloud top in RAMS (Appendix A, Fig. A1). These simulations show that the radiation parametrization significantly modifies the simulated liquid water content and can cause substantial differences between the models.

Figure 4 indicates a thicker cloud with a more stable cloud base when the number of accumulation mode aerosols increases. To clearly show the influence of Aitken mode particle concentration on simulated cloud microphysical properties, we have also shown the differences in cloud droplet, rain and total ice mixing ratios between each pair of simulations with the same accumulation mode concentration. These are discussed next (Sect. 3.3.1).

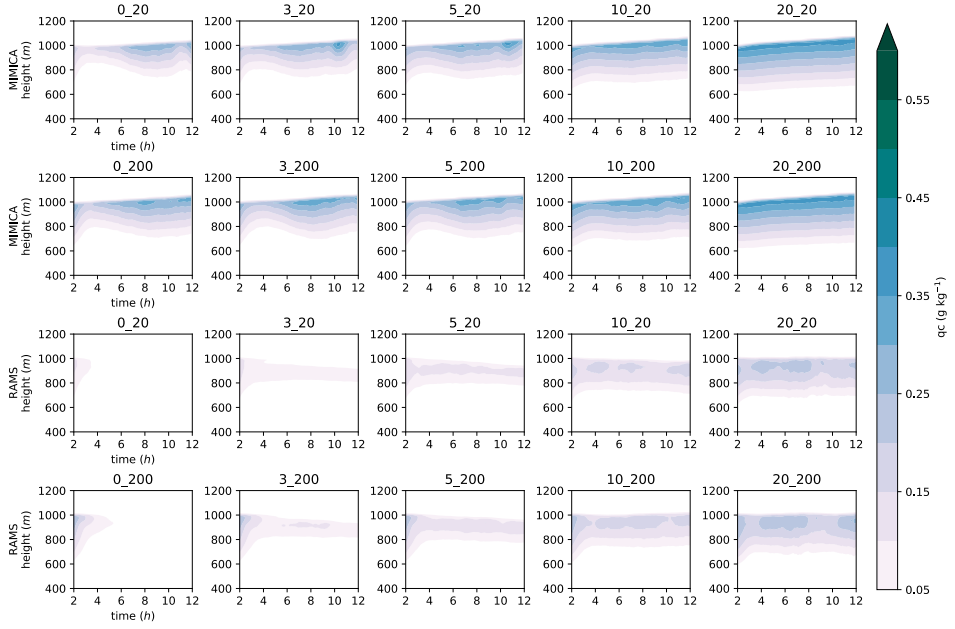

Figure 4: Cloud droplet mixing ratio (qc) for the MIMICA and RAMS simulation sets. The first 2 h of simulations are excluded from the plots as they are considered as a spin-up period. For figure clarity, the plot titles have been abbreviated; the first number refers to the accumulation mode and the second to the Aitken mode concentration in cm^{-3}, i.e. "0_20" refers to "AC0_AK20".

https://doi.org/10.5194/acp-2020-665
Preprint. Discussion started: 28 July 2020

Atmospheric Chemistry and Physics Discussions

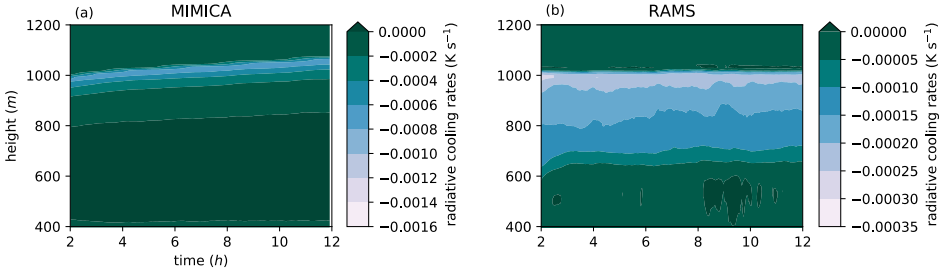

Figure 5. Radiative cooling rates in the baseline simulation (AC20_AK20), simulated by (a) MIMICA and (b) RAMS. The first 2 h of simulations are excluded as they are considered as a spin-up period.

3.3 Influence of Aitken mode particles

3.3.1 Influence of Aitken mode aerosol number concentration on cloud microphysical properties

Figure 6 shows that adding Aitken mode particles generally increases the amount of cloud droplet water in both models, i.e. the particles serve as CCN and allow formation of additional cloud droplets. The extent of their influence depends on the concentration of accumulation mode particles since these particles activate more easily and have the primary control on the cloud droplet concentration. A higher number of cloud droplets decreases the maximum supersaturation and available water vapor in the cloud. In MIMICA, the influence of smaller particles on cloud droplet mixing ratio decreases monotonically with increasing accumulation mode concentration (Fig. 5, top row). In RAMS, the cloud is very thin (or even dissipates) at low accumulation mode concentrations. Thus, there is no clear trend in the impact of the Aitken particles until the accumulation mode concentration is about 10 cm^{-3}, when there is a stable cloud (cf. Fig. 4). At concentrations higher than 10 cm^{-3} of accumulation mode particles, there is a similar trend in RAMS as in MIMICA, i.e. the influence of the Aitken mode becomes less pronounced with increasing accumulation mode particle concentration (Fig. 5, bottom row). The differences in cloud droplet mixing ratio are statistically significant (according to a student t-test with a 95 % confidence level on the time averages in the cloud layer) for all pairs of different Aitken mode concentrations in both models, except for the MIMICA pair AC20_AK200 and AC20_AK20. In other words, both models show that Aitken mode particles have a significant impact on the cloud droplet mixing ratio, at least up to 20 cm^{-3} of accumulation mode particles in RAMS and at least up to 10 cm^{-3} in MIMICA. The largest influence occurs in the uppermost part of the cloud (both in MIMICA and RAMS) where most of the cloud droplet water is present (cf. Fig. 4). The maximum difference at the very top of the cloud is mainly a result of higher cloud top heights in the simulations with a higher Aitken mode concentration (Fig. A3).

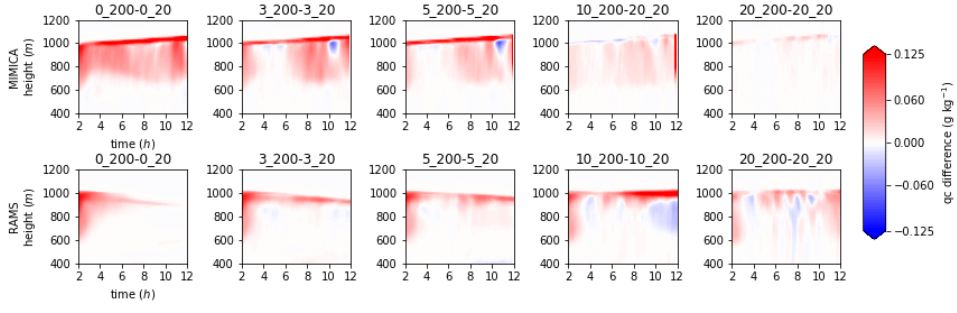

Figure 6: Differences in cloud droplet mixing ratio (qc) for simulation pairs with the same accumulation mode concentration (i.e. ACx_AK200-ACx_AK20) shown for MIMICA and RAMS. The first 2 h of simulations are excluded as they are considered as a spin-up period. A student's t-test with a 95% confidence level shows that the (time mean) differences are statistically significantly different for each pair of simulations, except for the pair AC20_AK200 and

https://doi.org/10.5194/acp-2020-665
Preprint. Discussion started: 28 July 2020

Atmospheric Chemistry and Physics Discussions

AC20_AK20 in MIMICA. For figure clarity, the plot titles have been abbreviated; the first number refers to the accumulation mode and the second to the Aitken mode concentration in cm^{-3}, i.e. "0_20" refers to "AC0_AK20".

Most of the rain water is present in the upper part of the cloud layer in all simulations with MIMICA (Fig. A4), in line with the maximum rain condensation rates shown for the baseline simulation (Fig. 3). In RAMS, the cases with higher accumulation mode concentrations, i.e. with a stable cloud, also show that most of the rain water is present close to the cloud top (Fig. A4). Figure 7 shows the effect of Aitken mode particles on rain water, i.e. comparing the pairs of simulations with the same accumulation mode concentrations. There are both positive and negative differences that vary with time in both models. At the beginning of the simulations, there is in general more rain produced in the cases with a higher number of Aitken mode particles (i.e. positive differences). Despite the higher number of cloud droplets, an increase in the Aitken mode particle concentration may lead to stronger turbulence and more cloud liquid water production, which could lead to stronger rain rates. Towards the end of the simulations, the rain rates are either about the same or there is less rain (i.e. negative differences). The presence of both positive and negative differences with time is a result of differences in cloud dynamics with different distributions of updrafts and downdrafts with time that govern the rain production in the cloud (cf. Fig. A9).

Differences in ice due to different Aitken mode concentrations are shown in Fig. 8 while total ice mixing ratios for all simulations are presented in Fig. A5. For the two lowest accumulation mode concentrations (0 and 3 cm^{-3}), there is in general more ice with a higher number of Aitken particles. In the cases with more accumulation mode particles (e.g., 5, 10, 20 cm^{-3}), the variability is larger with both positive and negative differences. This result can again be related to differences in cloud dynamics; a change in the Aitken mode particle number concentration results in that maximum updrafts are reached at somewhat different times. Differences are in general greater in MIMICA than in RAMS since there is a slightly more total ice in MIMICA (Fig. A5), but it is not possible to say which model is more realistic in terms of simulating the total ice amount (cf. Sect. 3.1).

We also tested the sensitivity of the simulated cloud properties to different Aitken mode particle concentrations for different levels of ice crystal concentrations using MIMICA (see Sect. 2). These simulations show that in clouds with more ice, the influence of the Aitken mode particles becomes lower for the liquid phase (Fig. A6).

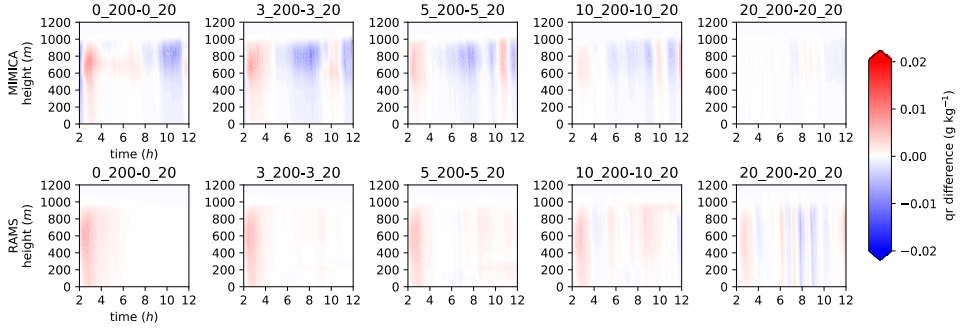

Figure 7: Differences in rain mixing ratio (qr) for simulation pairs with the same accumulation mode concentration (i.e. ACx_AK200-ACx_AK20) shown for MIMICA and RAMS. The first 2 h of simulations are excluded as they are considered as a spin-up period. A student's t-test with a 95% confidence level shows that the (time mean) differences are statistically significantly different for each pair of simulations except for the pair AC20_AK200 and AC20_AK20 in MIMICA. For figure clarity, the plot titles have been abbreviated; the first number refers to the accumulation mode and the second to the Aitken mode concentration in cm^{-3}, i.e. "0_20" refers to "AC0_AK20".

https://doi.org/10.5194/acp-2020-665
Preprint. Discussion started: 28 July 2020

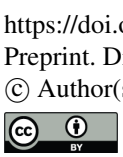

Atmospheric Chemistry and Physics Discussions

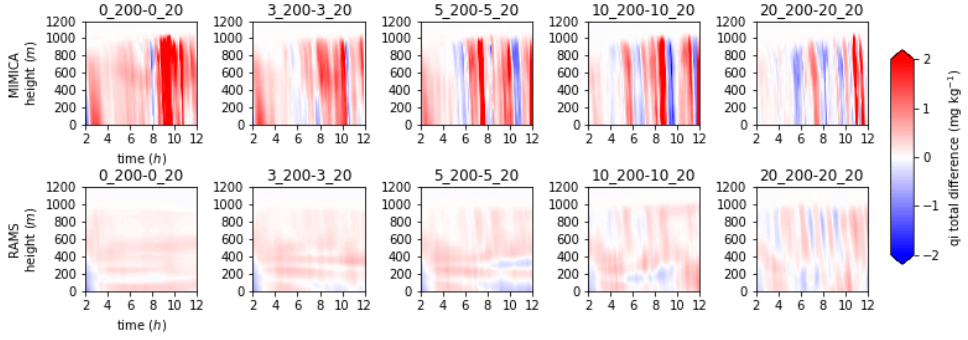

Figure 8: Differences in total ice mixing ratio (qi total) for simulation pairs with the same accumulation mode concentration (i.e. ACx_AK200-ACx_AK20) shown for MIMICA and RAMS. The first 2 h of simulations are excluded as they are considered as a spin-up period. A student's t-test with a 95% confidence level shows that the (time mean) differences are statistically significantly different in the first four pairs of simulations in both models. For figure clarity, the plot titles have been abbreviated; the first number refers to the accumulation mode and the second to the Aitken mode concentration in cm-3, i.e. "0_20" refers to "AC0_AK20".

3.3.2 Influence of Aitken mode aerosol hygroscopicity on cloud microphysical properties

Figure 9 shows that the change in the cloud droplet mixing ratio induced by Aitken mode particles increases as their κ-value increases, i.e. more hygroscopic Aitken mode particles lead to a larger increase in the cloud droplet amount. Higher particle hygroscopicity allows aerosol particle activation at lower supersaturations (see Sect. 4 for more information on supersaturation statistics).

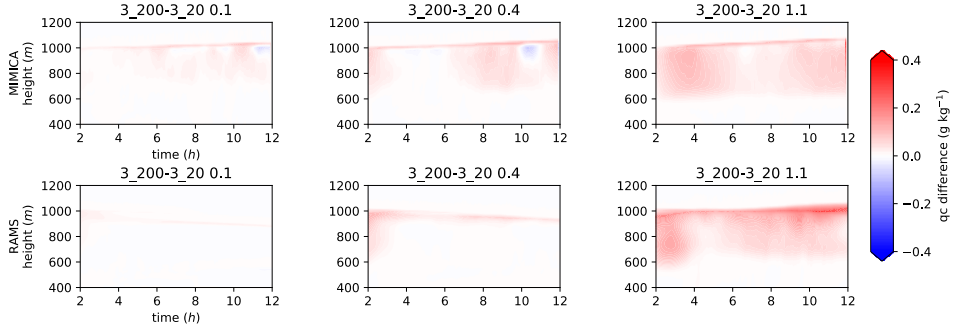

Figure 9: Differences in cloud droplet mixing ratio (qc) for simulation pairs with the same accumulation mode concentration and the same kappa value of the Aitken mode particles: =0.1 (the leftmost column); =0.4 (the middle column); =1.1 (the rightmost column) shown for MIMICA and RAMS. The first 2 h of simulations are excluded as they are considered as a spin-up period. A student's t-test with a 95% confidence level shows that the (time mean) differences are statistically significantly different for each pair of simulations. For figure clarity, the plot titles have been abbreviated; the first number refers to the accumulation mode and the second to the Aitken mode concentration in cm-3, i.e. "0_20" refers to "AC0_AK20".

The addition of Aitken mode particles with high κ-value leads to negative differences in rain amount in MIMICA, which can be explained by a greater number of cloud droplets and less efficient production of rain drops. However, in RAMS the differences are mostly positive, i.e. there is an increase in rain amounts (Fig. A7). The reason for this is most probably the very weak cloud layer produced by RAMS in the original AC3_AK20 simulation. As there is no cloud, there is also almost no precipitation - regardless of the κ-value. In both models, the impact of

https://doi.org/10.5194/acp-2020-665
Preprint. Discussion started: 28 July 2020

Atmospheric Chemistry and Physics Discussions

Aitken mode particles on the total ice mixing ratio generally becomes greater as the hygroscopicity of the particles increases (Fig. A8).

To summarize, the sensitivity tests show that Aitken mode particles can be activated even with a κ-value equal to 0.1 (more pronounced in MIMICA). Based on the model simulations, we can thus conclude that Aitken mode particles do not have to be highly hygroscopic in order to become CCN-active if accumulation mode aerosol concentrations are low.

4 Supersaturation statistics

We analyze next the simulated water vapor supersaturation (ss) values reached within the model domains in order to investigate how the ss statistics depend on different prescribed aerosol size distributions as well as on different hygroscopic properties of the Aitken mode particles. The ss statistics have been calculated for a 20min period around 6 h of simulation for all the cases simulated with the default κ-value (κ=0.4; i.e. dependence on the aerosol size distribution, Fig. 10). They have also been calculated for the AC3_AK20 and AC3_AK200 simulations initialized with different κ-values for the Aitken mode particles (κ=[0.1,1.1]; i.e. dependence on the hygroscopic properties, Fig. 11). In figure 10, the median ss values in both models generally vary between 0.2 and 0.4 %. The exception is the case AC0_AK20 in RAMS where there is no stable cloud at 6 h. The ss values in this simulation are high since the statistics are based on a relatively low number of supersaturated grid boxes, which in this case reach high ss values due to a low condensational sink. The median numbers agree well with typical ss values reported for clean marine stratocumulus clouds at mid-latitudes (Hudson and Noble, 2014; Yang et al., 2019). However, the 99_{th} percentiles show high supersaturations with values above 1 % for most of the simulations. As expected, simulated ss values decrease with higher accumulation mode number concentration. They are even lower when the Aitken mode concentration is prescribed to a larger number (200 vs. 20 cm^{-3}). The median values in Fig. 11 also vary between 0.2 and 0.4 % and in general decrease with a higher κ-value of the Aitken mode particles for the two tested concentrations in both MIMICA and RAMS. Again, the 99_{th} percentiles show high values that exceed 1 % in most of the cases.

The numbers shown in Fig. 10 and Fig. 11 are the critical dry diameters calculated for the 75_{th} and 99_{th} percentiles of the ss values (cf. Fig. A10). These values can be generally compared with the mean diameter of 32 nm prescribed for the Aitken mode in this study. Our analysis confirms that supersaturations within the model domains reach high enough values to activate Aitken mode particles for all tested accumulation mode concentrations and all tested Aitken mode κ-values. The results also agree well with recent findings for the region south of the ice edge during the summertime, which have shown that particles smaller than the accumulation mode potentially can act as CCN (i.e. smaller than 50 nm in diameter; Willis et al., 2016; Kecorius et al., 2019; Koike at al., 2019). If the calculations in Fig. A10 are done for higher (lower) surface tension, the maximum ss values would need to be higher (lower) to activate particles of the same critical dry diameters as the ones presented here.

Updraft statistics calculated for the same time period as the ss statistics for the set of cases simulated with the default κ-value show that the updrafts are in general stronger with increasing accumulation mode concentration (Fig. A9). The statistical values generally cover a range of updrafts between 0 to 1 ms^{-1}, which agrees well with the vertically resolved updraft estimates by Sedlar and Shupe (2014) for the ASCOS campaign. With an increase in accumulation mode particles, there is more vapor condensation and thus more liquid water in the cloud that drives the turbulence through cloud-top radiative cooling. Stronger turbulence further leads to stronger updrafts and further condensation.

https://doi.org/10.5194/acp-2020-665
Preprint. Discussion started: 28 July 2020

Atmospheric Chemistry and Physics Discussions

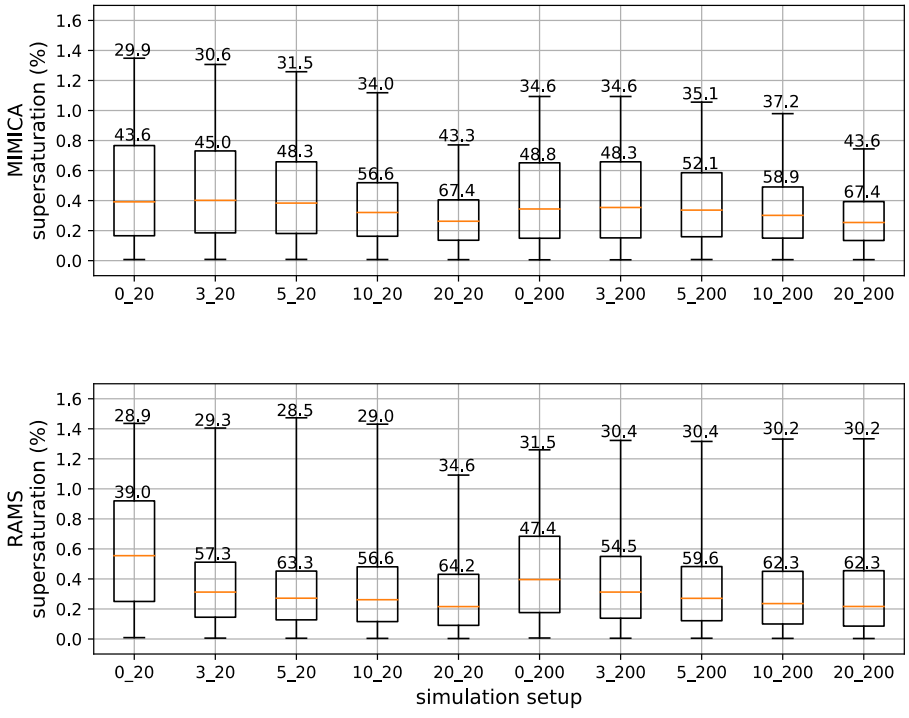

520

Figure 10: Supersaturation statistics shown for a set of cases initialized with a κ-value of 0.4, simulated by MIMICA and RAMS. The statistics are calculated for a 20min period around 6 h of simulation for all grid boxes with relative humidity > 100 %. Lower and upper whiskers correspond to 1st and 99th percentiles, respectively. The numbers written in the figure are critical dry diameters that correspond to supersaturation 75th percentiles (upper limit of the box) and 99th percentiles. For figure clarity, the plot titles have been abbreviated; the first number refers to the accumulation mode and the second to the Aitken mode concentration in cm-3, i.e. "0_20" refers to "AC0_AK20".

525

https://doi.org/10.5194/acp-2020-665
Preprint. Discussion started: 28 July 2020

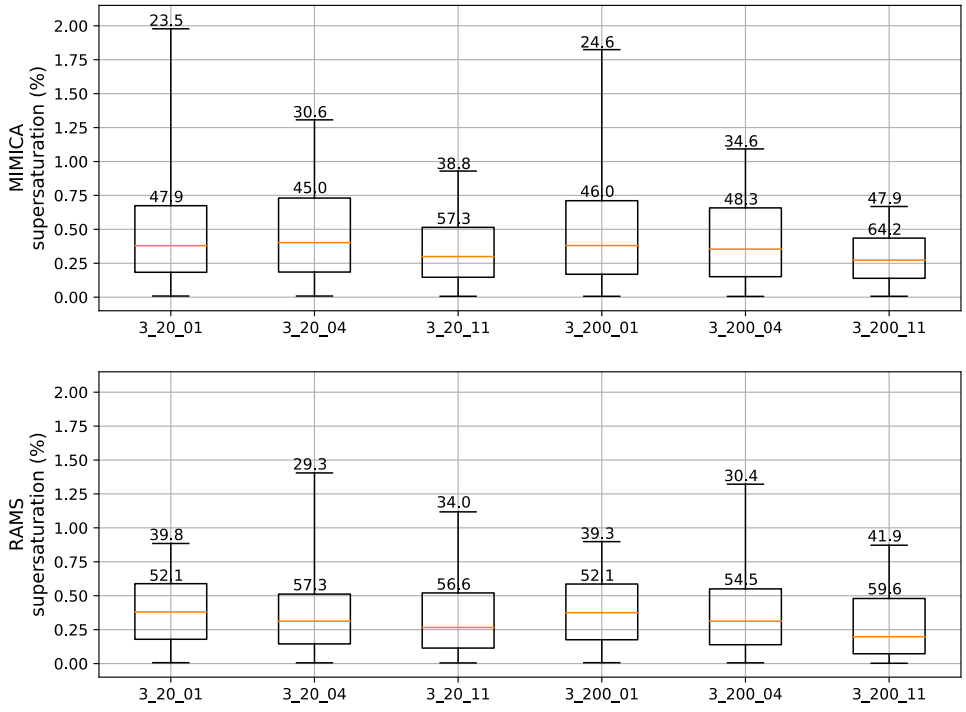

Figure 11. Supersaturation statistics shown for the simulations AC3_AK20 and AC3_AK200 initialized with different κ-values = [0.1, 0.4, 1.1], simulated by MIMICA and RAMS. The statistics are calculated for a 20min period around 6 h of simulation for all grid boxes with relative humidity > 100 %. Lower and upper whiskers correspond to 1st and 99th percentiles, respectively. The numbers written in the figure are critical dry diameters that correspond to supersaturation 75th percentiles (upper limit of the box) and 99th percentiles. For figure clarity, the plot titles have been abbreviated; the first number refers to the accumulation mode and the second to the Aitken mode concentration in cm-3, i.e. "3_20_01" refers to "AC3_AK20" initialized with a κ-value=0.1.

5 Qualitative comparison of model results with observational data for the High Arctic

Both models suggest that Aitken mode particles are important as CCN in high Arctic SMP clouds if accumulation mode concentrations are low. Guided by these analyses we have revisited the observed aerosol size distributions from four high Arctic expeditions, including the ASCOS campaign (Leck et al., 1996; Leck et al., 2001; Leck et al., 2004; Tjernström et al., 2014). We first examined the representativeness of the size distributions that we have applied in our simulations, i.e. how frequently these types of distributions occur in the observations. Fig. 12 shows two classes of size distributions: one with Aitken mode concentrations lower than 25 cm-3 (AIT < 25 cm-3, blue line) and one with Aitken mode concentrations between 100<AIT<200 cm-3 (orange line). The cases with accumulation mode number concentrations equal to 20 cm-3 (i.e. the maximum accumulation mode concentration prescribed in the simulations) have the occurrence probability of 5 % and 17 % (of total minutes of observations) for the class 100<AIT<200 cm-3 and AIT < 25 cm-3, respectively. This means that in conditions with low accumulation mode concentrations (i.e. lower than 20 cm-3) there is a higher probability for the Aitken mode particle concentration to also be low in number (i.e. lower than ~25 cm-3). However, it also happens that Aitken mode concentrations are much higher (>~100 cm-3). In other words, the prescribed size distributions that we have applied in our simulations are reasonable.

Probability density functions (PDFs) of observed Hoppel diameters (Hoppel et al., 1986; Fig. 13), calculated as detailed in Heintzenberg and Leck (2012), show that the PDFs for all four expeditions peak around 60 nm, i.e. this should be the most common activation diameter. However, the smallest observed Hoppel diameters are around 40 nm, supporting our conclusions that small Aitken mode particles may be activated in the high Arctic under certain

https://doi.org/10.5194/acp-2020-665
Preprint. Discussion started: 28 July 2020

Atmospheric Chemistry and Physics Discussions

conditions. The observational statistics agree well with the calculations of the critical dry diameters obtained from the simulated ss values (Sect. 4).

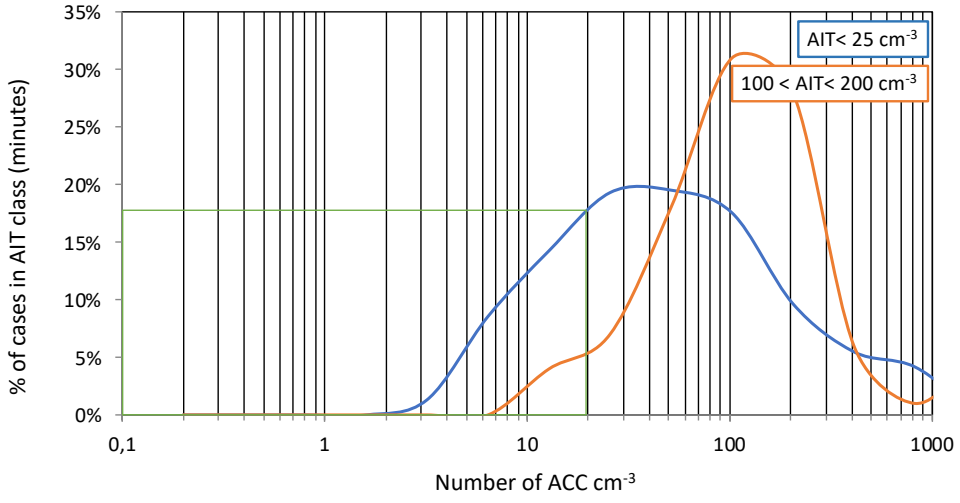

Figure 12. The occurrence probability (% of total minutes of observations) for two classes of Aitken (AIT) mode concentrations: AIT < 25 cm^{-3} and 100<AIT<200 cm^{-3}. On the x-axis is the number of accumulation (ACC) mode particles in cm^{-3}. The statistics are calculated for four different expeditions in the high Arctic, in the summers of 1991, 1996, 2001 and 2008. Further details on the quality and data processing of the aerosol size resolved measurements are available in Heintzenberg and Leck (2012).

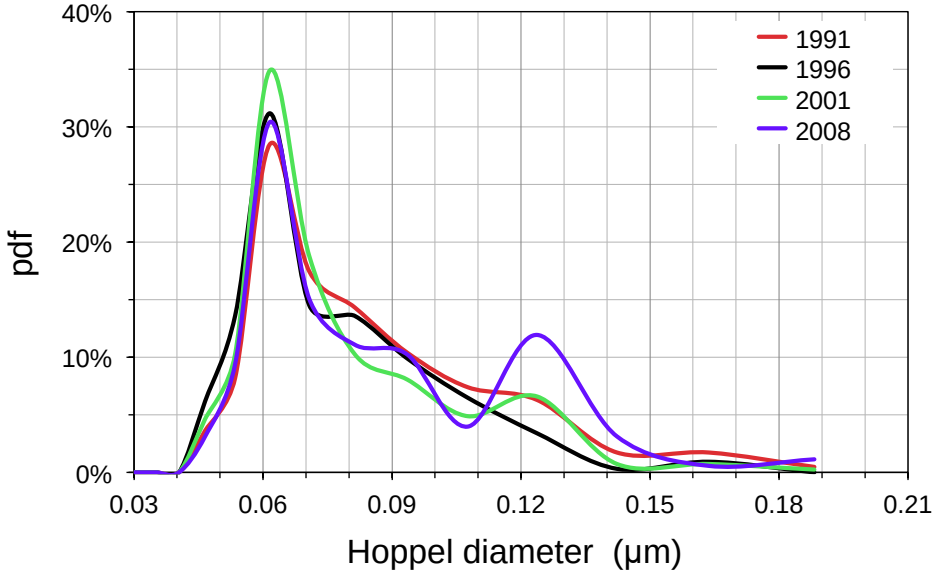

Figure 13: Probability density function (pdf) of the Hoppel diameter shown for four different expeditions in the high Arctic, in the summers of 1991, 1996, 2001 and 2008. Further details on the quality and data processing of the aerosol size resolved measurements are available in Heintzenberg and Leck (2012).

https://doi.org/10.5194/acp-2020-665
Preprint. Discussion started: 28 July 2020

Atmospheric Chemistry and Physics Discussions

6 Summary and conclusions

This study investigates the potential importance of Aitken mode particles in sustaining and affecting the properties of stratiform mixed-phase clouds in the high Arctic. To perform such a task, we have used two LES models (MIMICA and RAMS) to simulate a summertime high Arctic SMP cloud observed during the ASCOS campaign (Tjernström et al., 2014) and initialized the models with different aerosol size distributions. Both models show that Aitken mode aerosols have a significant impact on the cloud droplet amount, if the accumulation mode number concentration is less than 10–20 cm^{-3}. Simulations performed with different values of the hygroscopicity parameter κ indicate that more hygroscopic Aitken mode particles lead to a higher number of cloud droplets, as expected. Moreover, the simulations show that Aitken mode particles can act as CCN and influence the properties of SMP clouds even at the low κ-values (=0.1). If the ice fraction of the SMP cloud is high (i.e. ice-rich clouds), the influence of Aitken mode particles on the liquid phase decreases.

Both models are in qualitative agreement in terms of the influence of Aitken mode particles on cloud properties, even though the models show different results regarding e.g., the relative role of different microphysical processes and the simulated amount of LWP. The most striking difference in modelled cloud properties between the two models appears to be caused by the difference in radiation schemes. RAMS produces less radiative cooling for a certain amount of cloud water compared to MIMICA and does not sustain a cloud at low accumulation mode aerosol concentrations (<3–10 cm^{-3}). The radiative cooling rates produced by MIMICA agree better with the observation-based estimates (Brooks et al., 2017), however, the observations are in general not sufficient to constrain or rank the models in terms of their performance. This would require additional observations (of e.g., cloud-top radiative cooling rates, updrafts, supersaturations) and less uncertainty in the retrieved data (of e.g., LWP and IWP).

The simulated median supersaturations in both MIMICA and RAMS vary between 0.2 and 0.4 %, but values above 1 % were also found within the model domains (99^{th} percentile values). The spatial variability in the simulated supersaturations and updrafts demonstrates the potential issue of applying constant supersaturation values for a grid box, or even a certain cloud type, within e.g., general circulation models. Calculations of threshold diameters of aerosol activation confirm that the simulated supersaturation values are high enough for Aitken mode particles to be activated (i.e. the activation diameter is as low as ~30 nm). Furthermore, statistics of the observed Hoppel minimum diameter from four different expeditions in the high Arctic (Heintzenberg and Leck, 2012) also suggest that aerosols in the Aitken mode are activated as CCN. Our results also agree well with the recent studies for the lower Arctic, which have inferred the importance of particles smaller than 50 nm as potential CCN (Willis et al., 2016; Kecorius et al., 2019; Koike at al., 2019).

Our findings highlight the importance of better understanding Aitken mode particle formation, chemical properties and emissions, in particular in pristine environments such as the high Arctic in summer. They also show that accumulation mode particles should not be considered as the only potential CCN in models, as this may lead to e.g., too low background CCN concentrations and too high estimates of anthropogenic aerosol indirect effects.

https://doi.org/10.5194/acp-2020-665
Preprint. Discussion started: 28 July 2020

Atmospheric Chemistry and Physics Discussions

Appendix A:

The cloud droplet mixing ratio simulated by the two models using different radiative transfer schemes is shown in Fig. A1. Using simple radiative transfer schemes (i.e. radiation_simple simulations; the radiative fluxes depend on LWP only, Stevens et al. (2005) in MIMICA and Chen and Cotton (1983) in RAMS) instead of the default radiation solvers (radiation_solver simulations; Fu and Liou (1993) in MIMICA and Harrington (1997) in RAMS) leads to a lower cloud water amount and a thinner cloud in MIMICA compared to RAMS, i.e. the opposite result compared to when using the default radiation solvers. Another test where the radiative cooling rates within RAMS were multiplied by a factor of 5 at the top of the cloud produces a much thicker cloud than the one in the MIMICA radiation_solver simulation, which confirms that the cooling efficiency of the radiative scheme is a critical factor for determining the cloud droplet amount and consequently also the cloud lifetime. The results show that the radiation parametrization used in the model has a significant impact on the simulated cloud properties and is especially important to be considered in model intercomparison studies.

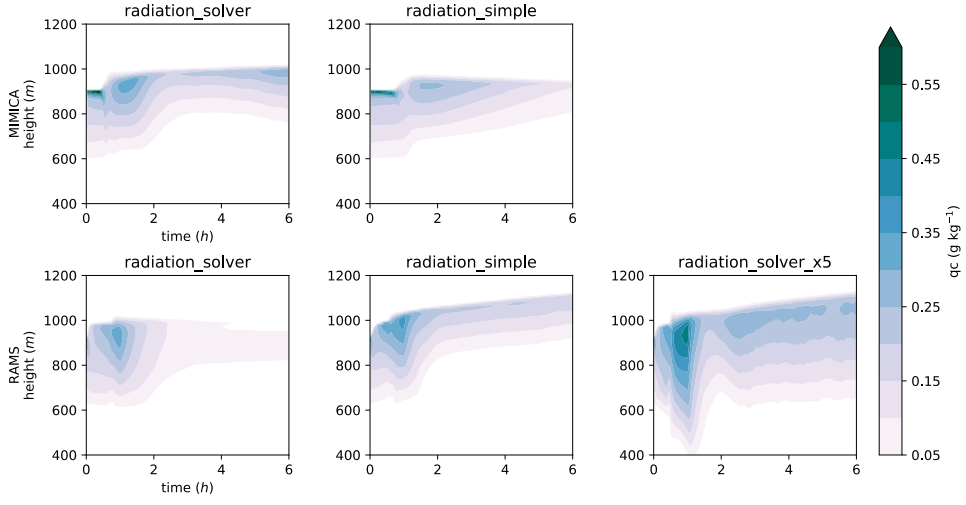

Figure A1: Cloud droplet mixing ratio (qc) shown for a simulation AC3_AK20 initialized with different radiative schemes in MIMICA and RAMS. The title *radiation_solver* is used for the simulations where the models are initialized with their default radiation solvers (Fu and Liou (1993) in MIMICA and Harrington (1997) in RAMS). The title *radiation_simple* is used for the simulations where the radiative fluxes are calculated as functions of LWP only (Stevens et al. (2005) in MIMICA and Chen and Cotton (1983) in RAMS). The *radiation_solver_x5* simulated by RAMS shows the qc obtained with the default radiation solver but with a 5x higher cooling rate enforced at cloud top. The simulations are run for 6 h.

https://doi.org/10.5194/acp-2020-665
Preprint. Discussion started: 28 July 2020

Atmospheric Chemistry and Physics Discussions

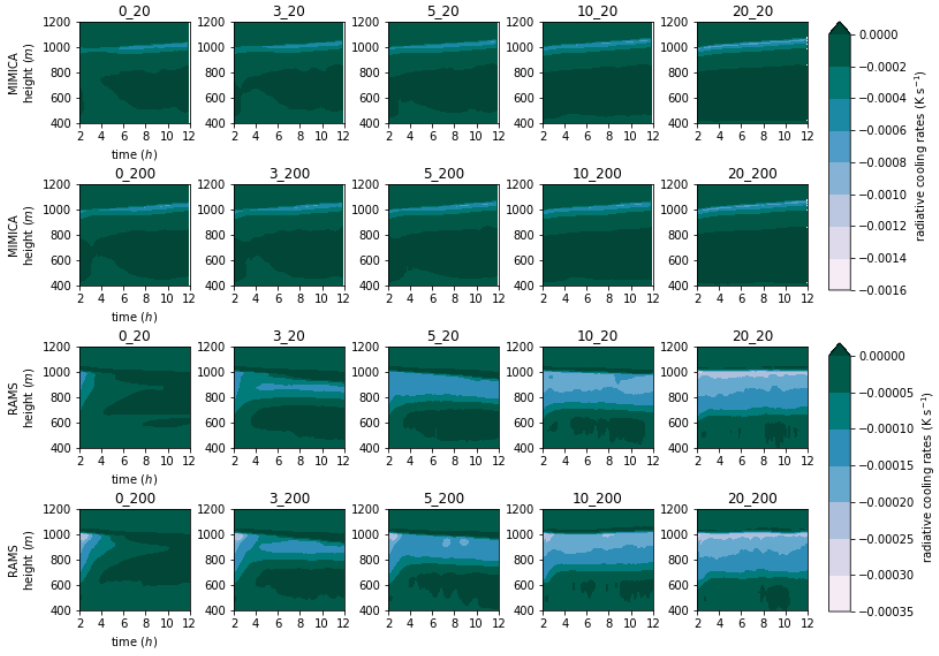

Figure A2: Radiative cooling rates for the MIMICA and RAMS simulation sets. The first 2 h of simulations are excluded from the plots as they are considered as a spin-up period. For figure clarity, the plot titles have been abbreviated; the first number refers to the accumulation mode and the second to the Aitken mode concentration in cm-3, i.e. "0_20" refers to "AC0_AK20".

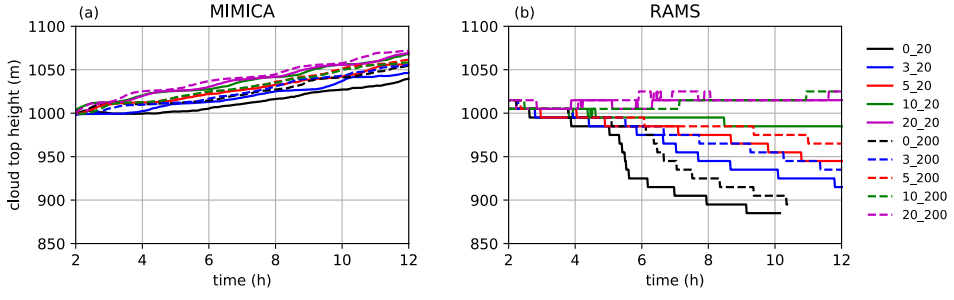

Figure A3: Cloud top heights in (a) MIMICA and (b) RAMS. The first 2 h of simulations are excluded from the plots as they are considered as a spin-up period.

https://doi.org/10.5194/acp-2020-665
Preprint. Discussion started: 28 July 2020

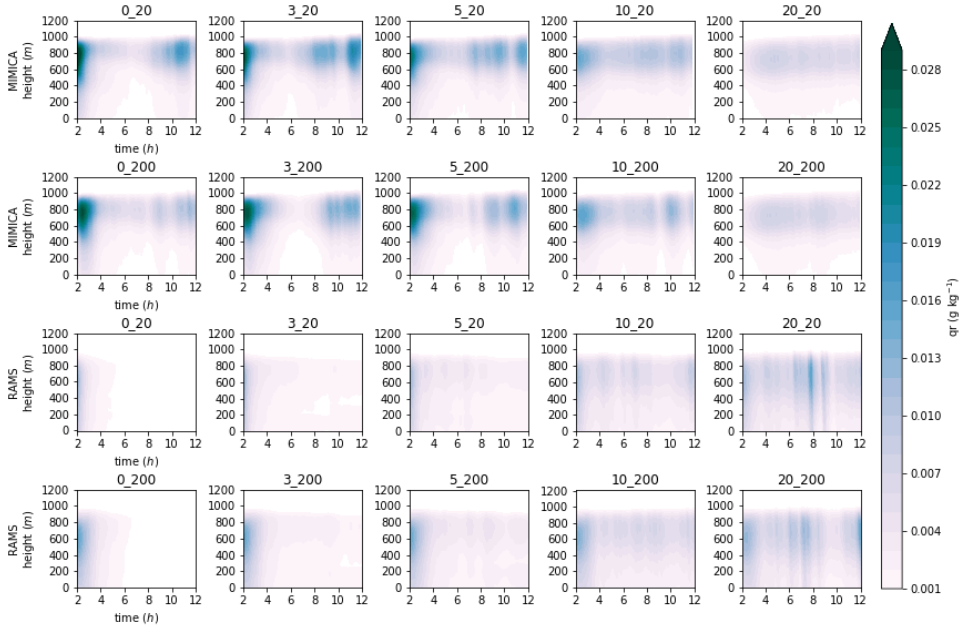

685 **Figure A4: Rain mixing ratio (qr) for the MIMICA and RAMS simulation sets. The first 2 h of simulations are excluded from the plots as they are considered as a spin-up period. For figure clarity, the plot titles have been abbreviated; the first number refers to the accumulation mode and the second to the Aitken mode concentration in cm-3, i.e. "0_20" refers to "AC0_AK20".**

https://doi.org/10.5194/acp-2020-665
Preprint. Discussion started: 28 July 2020

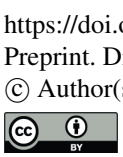

Atmospheric Chemistry and Physics Discussions

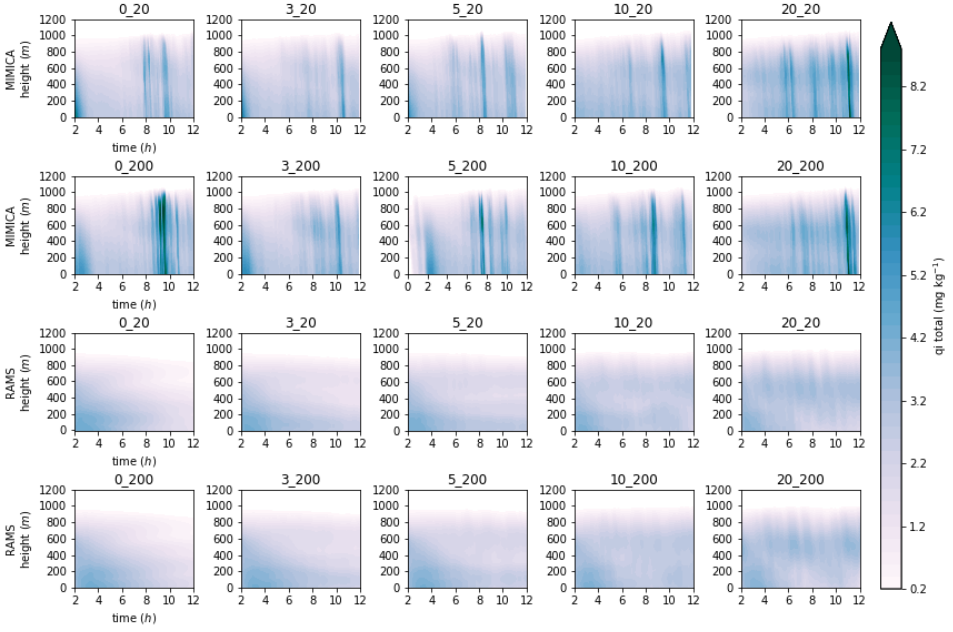

690

Figure A5: Total ice mixing ratio (qi total) for the MIMICA and RAMS simulation sets. The first 2 h of simulations are excluded from the plots as they are considered as a spin-up period. For figure clarity, the plot titles have been abbreviated; the first number refers to the accumulation mode and the second to the Aitken mode concentration in cm-3, i.e. "0_20" refers to "AC0_AK20".

695

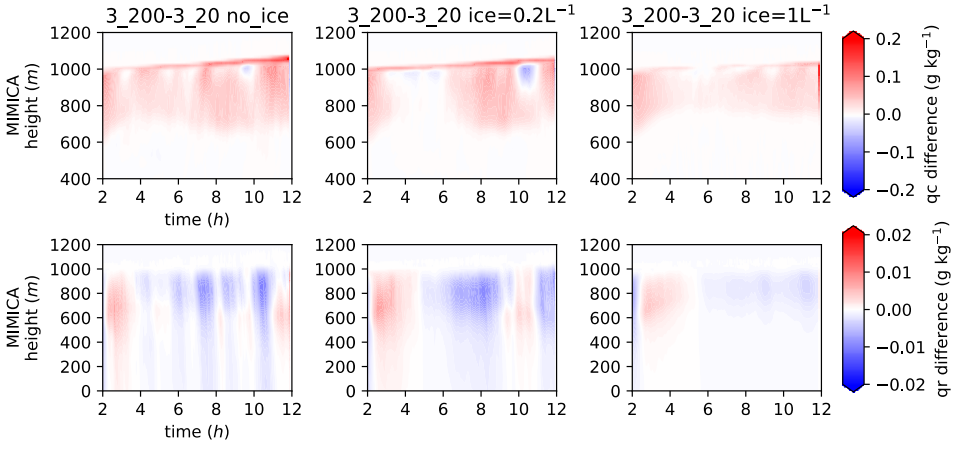

700

Figure A6: Differences in cloud water mixing ratio (qc) and rain mixing ratio (qr) for simulation pairs with the same accumulation mode concentration and the same ice crystal concentration: =0 L-1 (no_ice, the leftmost column); =0.2 L-1 (the middle column); =1 L-1 (the rightmost column) shown for MIMICA. The first 2 h of simulations are excluded as they are considered as a spin-up period. A student's t-test with a 95% confidence level shows that the (time mean) differences are statistically significantly different for each pair of simulations. For figure clarity, the plot titles have

705

https://doi.org/10.5194/acp-2020-665
Preprint. Discussion started: 28 July 2020

Atmospheric Chemistry and Physics Discussions

been abbreviated; the first number refers to the accumulation mode and the second to the Aitken mode concentration in cm^{-3}, i.e. "3_20" refers to "AC3_AK20".

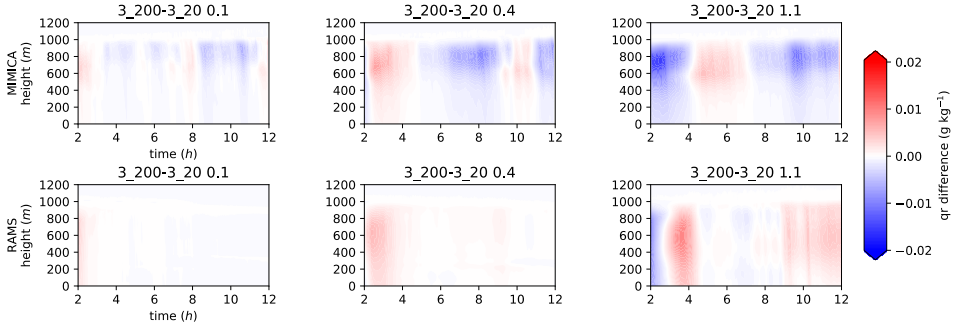

Figure A7: Differences in rain mixing ratio (qr) for simulation pairs with the same accumulation mode concentration and the same kappa value of the Aitken mode particles: =0.1 (the leftmost column); =0.4 (the middle column); =1.1 (the rightmost column) shown for MIMICA and RAMS. The first 2 h of simulations are excluded as they are considered as a spin-up period. A student's t-test with a 95% confidence level shows that the (time mean) differences are statistically significantly different for each pair of simulations. For figure clarity, the plot titles have been abbreviated; the first number refers to the accumulation mode and the second to the Aitken mode concentration in cm^{-3}, i.e. "3_20" refers to "AC3_AK20".

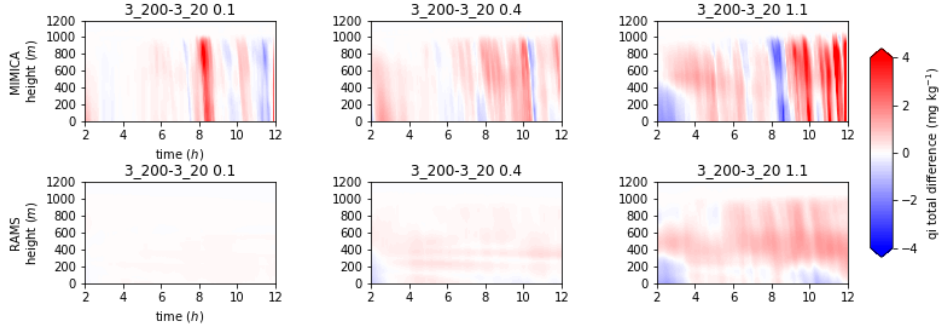

Figure A8: Differences in total ice mixing ratio (qi total) for simulation pairs with the same accumulation mode concentration and the same kappa value of the Aitken mode particles: =0.1 (the leftmost column); =0.4 (the middle column); =1.1 (the rightmost column) shown for MIMICA and RAMS. The first 2 h of simulations are excluded as they are considered as a spin-up period. A student's t-test with a 95% confidence level shows that the (time mean) differences are statistically significantly different for each pair of simulations. For figure clarity, the plot titles have been abbreviated; the first number refers to the accumulation mode and the second to the Aitken mode concentration in cm^{-3}, i.e. "3_20" refers to "AC3_AK20".

https://doi.org/10.5194/acp-2020-665
Preprint. Discussion started: 28 July 2020

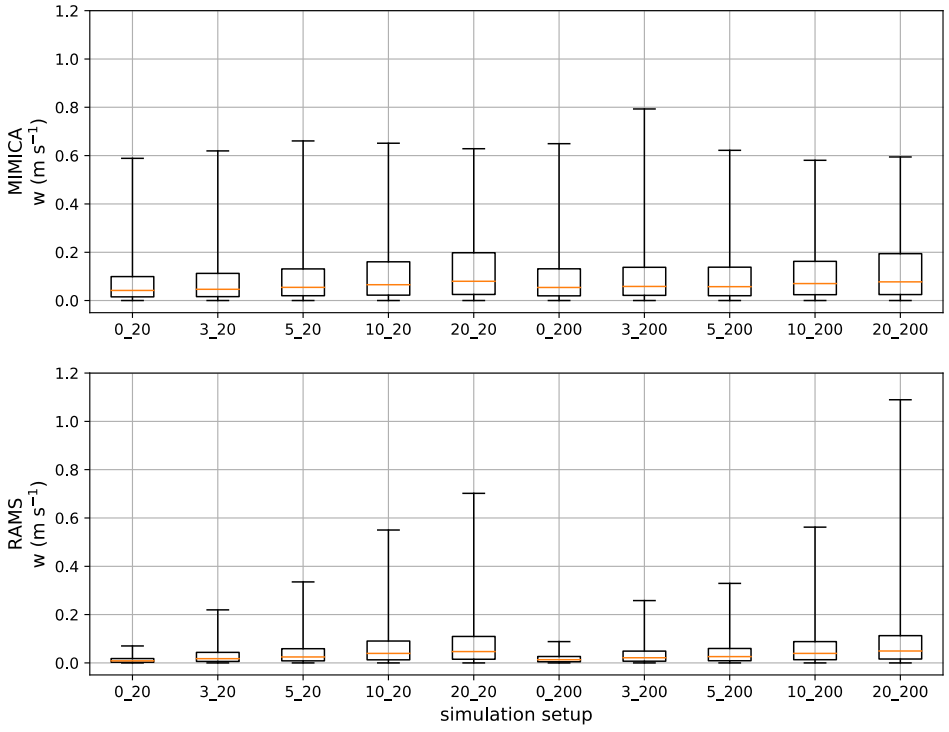

740 **Figure A9: Updraft (w) statistics shown for a set of cases, simulated by MIMICA and RAMS. Lower and upper whiskers correspond to 1st and 99th percentiles, respectively. For figure clarity, the plot titles have been abbreviated; the first number refers to the accumulation mode and the second to the Aitken mode concentration in cm-3, i.e. "0_20" refers to "AC0_AK20".**

745 Figure A10 shows the relationship between critical supersaturation and dry diameters calculated for a range of kappa values, i.e. κ=[0.1; 0.2; 0.3; 0.4; 0.5; 0.6; 0.7; 0.8; 0.9; 1.0; 1.1]. The computation is done for the temperature T=298.15 K and the surface tension σs/a=0.072 Jm–2. More details on the calculations can be found in Petters and Kreidenweis (2007).

750

https://doi.org/10.5194/acp-2020-665
Preprint. Discussion started: 28 July 2020

Atmospheric Chemistry and Physics Discussions

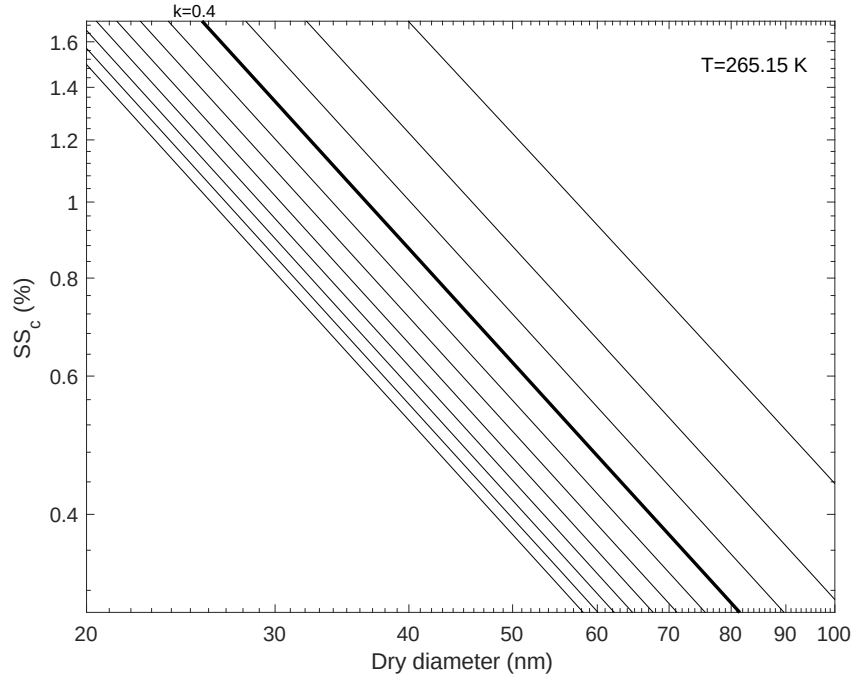

Figure A10: Calculated critical supersaturations SSc (%) as a function of dry diameter, computed for σs/a=0.072 J m^{-2} and T=298.15 K. κ-lines are shown for a range 0.1 ≤ κ ≤ 1.1. Bold line corresponds to kappa=0.4.

760

765 *Data availability.* Modelling datasets used in this study are available at https://bolin.su.se/data/bulatovic-2020 with assigned doi (https://doi.org/10.17043/bulatovic-2020). The observational datasets are available from corresponding authors upon request.

Author contribution. IB, ALI and AMLE designed the experiments. IB and ALI performed the model simulations.
770 IB analyzed the datasets. CL and JH provided the figures in the section "Qualitative comparison of model results with observational data for the High Arctic". IB prepared the manuscript with contributions from all co-authors.

Competing interests. The authors declare that they have no conflict of interest.

775 *Acknowledgements.* AMLE acknowledges the Swedish Science Foundation (Vetenskapsrådet), grant 2015-05318. ALI acknowledges the U.S. Department of Energy's Atmospheric System Research Grant DE-SC0019073. CL acknowledges Swedish Research Council (project no. 2016-03518, Leck). IR acknowledges Knut and Alice Wallenberg Foundation (Wallenberg Academy Fellowship project AtmoRemove 2015.0162) and European Commission (H2020 project FORCeS, grant agreement No 821205 and ERC-CoG project INTEGRATE, grant
780 agreement No 865799). IB gratefully acknowledges Knut and Alice Wallenberg foundation for a scholarship from the Anniversary Travel Grants and the Bolin Centre Research group 2 for travel funds. The computations performed using MIMICA and data handling were enabled by resources provided by the Swedish National Infrastructure for Computing (SNIC) at the National Supercomputer Centre (NSC) partially funded by the Swedish Research Council through grant agreement no. 2016-07213.

785

https://doi.org/10.5194/acp-2020-665
Preprint. Discussion started: 28 July 2020

Atmospheric Chemistry and Physics Discussions

References

Bigg, E. K. and Leck, C: Cloud-active particles over the central Arctic ocean, J. Geophys. Res., 106 (D23), 32, 155-32, 166, https://doi.org/10.1029/1999JD901152, 2001.

Bigg, E. K., Leck, C., and Nilsson, E. D.: Sudden changes in arcticatmospheric aerosol concentrations during summer and autumn, Tellus, 48B, 254–271, https://doi.org/10.3402/tellusb.v48i2.15890, 1996.

Birch, C. E., Brooks, I. M., Tjernström, M., Shupe, M. D., Mauritsen, T., Sedlar, J., Lock, A. P., Earnshaw, P., Persson, P. O. G., Milton, S. F., and Leck, C.: Modelling atmospheric structure, cloud and their response to CCN in the central Arctic: ASCOS case studies, Atmos. Chem. Phys., 12, 3419–3435, https://doi.org/10.5194/acp-12-3419-2012 , 2012.

Brooks, I. M., Tjernström, M., Persson, P.O.G., Shupe, M. D., Atkinson, R. A., Canut, G., Birch, C. E., Mauritsen, T., Sedlar. J., and Brooks, B. J.: The turbulent structure of the Arctic summer boundary layer during the Arctic summer cloud-ocean study, J. Geophys. Res. Atmos., 122, 9685–9704, https://doi.org/10.1002/2017JD027234, 2017.

Bulatovic, I. and Igel, A. L.: Data from a modelling study on the importance of Aitken mode particles for cloud sustenance in the high Arctic, https://doi.org/10.17043/bulatovic-2020, 2020.

Chen, C. and Cotton, W. R.: A one-dimensional simulation of the stratocumulus-capped mixed layer, Bound.-Layer Meteor., 25, 289-321, 1983.

Christiansen, S., Ickes, L., Bulatovic, I., Leck, C., Murray, B. J., Bertram, A. K., Wagner, R., Gorokhova, E., Salter, M. E., Ekman, A. M. L., and Bilde, M.: Influence of Arctic microlayers and algal cultures on sea spray hygroscopicity and the possible implications for mixed-phase clouds, J. Geophys. Res. Atmos, in review.

Cotton, W. R., Pielke Sr., R. A., Walko, R. L., Liston, G. E., Tremback, C. J., Jiang, H., McAnelly, R. L., Harrington, J. Y., Nicholls, M. E., Carrio, G. G., and McFadden, J. P.: RAMS 2001: Current status and future directions, Meteorol. Atmos. Phys., 82, 5–29, https://doi.org/10.1007/s00703-001-0584-9, 2003.

Covert, D. S., Wiedensohler, A., Aalto, P., Heintzenberg, J., McMurry, P. H., and Leck, C.: Aerosol number size distributions from 3 to 500 nm diameter in the arctic marine boundary layer during summer and autumn, Tellus, 48B, 197-212, https://doi.org/10.3402/tellusb.v48i2.15886, 1996.

Curry, J. A. and Ebert, E. E.: Annual cycle of radiative fluxes over the Arctic Ocean: Sensitivity to cloud optical properties. J. Climate, 5, 1267–1280, https://doi.org/10.1175/1520-0442(1992)005<1267:ACORFO>2.0.CO;2, 1992.

Curry, J. A., Rossow, W.B., Randall, D., and Schramm, J. L.: Overview of Arctic cloud and radiation characteristics. J. Climate, 9, 1731–1764, https://doi.org/10.1175/1520-0442(1996)009<1731:OOACAR>2.0.CO;2, 1996.

Dimitrelos, A., Ekman, A. M. L., Caballero, R., and Savre, J.: A Sensitivity Study of Arctic Air-Mass Transformation Using Large Eddy Simulation, 125, e2019JD031738, https://doi.org/10.1029/2019JD031738, 2020.

Ekman, A. M. L., Wang, C., Ström, J., and Krejci, R.: Explicit simulation of aerosol physics in a cloud-resolving model: Aerosol transport and processing in the free troposphere, J. Atmos. Sci., 63(2), 682–696, https://doi.org/10.1175/JAS3645.1, 2006.

Feingold, G., Boers, R., Stevens, B., and Cotton, W. R.: A modeling study of the effect of drizzle on cloud optical depth and susceptibility. J. Geophys. Res., 102, 13527, https://doi.org/10.1029/97JD00963, 1997.

Fu, Q. and Liou, K. N.: Parameterization of the radiative properties of cirrus clouds, J. Atmos. Sci., 50, 2008–2025, https://doi.org/10.1175/1520-0469(1993)050<2008:POTRPO>2.0.CO;2, 1993.

https://doi.org/10.5194/acp-2020-665
Preprint. Discussion started: 28 July 2020

Atmospheric Chemistry and Physics Discussions

Garrett, T. J., Radke, L. F., and Hobbs, P. V.: Aerosol Effects on Cloud Emissivity and Surface Longwave Heating in the Arctic, J. Atmos. Sci., 59, 769-778, https://doi.org/10.1175/1520-0469(2002)059<0769:AEOCEA>2.0.CO;2, 2002.

Garrett, T., Maestas, M. M., Krueger, S. K., and Schmidt, C. T.: Acceleration by aerosol of a radiative-thermodynamic cloud feedback influencing Arctic surface warming, Geophys. Res. Lett., 36, L19804, https://doi.org/10.1029/2009GL040195, 2009.

Ghan, S., J., Leung, R., L., Easter, R. C., and Abdul-Razzak, H.: Prediction of cloud droplet number in a general circulation model, J. Geophys. Res., 102(D18), 21,777-21,794, https://doi.org/10.1029/97JD01810, 1997.

Harrington, J. Y.: The effects of radiative and microphysical processes on simulation of warm and transition season Arctic stratus, Colorado State University, 289 pp, 1997.

Hartmann, D. L., Klein Tank, A. M. G., Rusticucci, M., Alexander, L. V., Brönnimann, S., Charabi, Y. A. R., Dentener, F. J., Dlugokencky, E. J., Easterling, D. R., Kaplan, A., Soden, B. J., Thorne, P. W., Wild, M., and Zhai, P. M.: Observations: Atmosphere and Surface, in: Climate change 2013: The physical science basis. Contribution of Working Group I to the Fifth Assessment Report of the Intergovernmental Panel on Climate Change, edited by: Stocker, T. F., Qin, D., Plattner, G.-K., Tignor, M., Allen, S. K., Boschung, J., Nauels, A., Xia, Y., Bex V., and Midgley, P. M., Cambridge University Press, Cambridge, United Kingdom and New York, NY, USA, 159–254, https://doi.org/10.1017/CBO9781107415324.008, 2013.

Heintzenberg, J. and Leck, C.: The summer aerosol in the central Arctic 1991–2008: did it change or not?, Atmos. Chem. Phys., 12, 3969–3983, https://doi.org/10.5194/acp-12-3969-2012, 2012.

Heintzenberg, J., Leck, C., and Tunved P.: Potential source regions and processes of aerosol in the summer Arctic, Atmos. Chem. Phys., 15, 6487–6502, https://doi.org/10.5194/acp-15-6487-2015, 2015.

Holland, M. M. and Bitz, C. M.: Polar amplification of climate change in coupled models, Clim. Dyn., 21, 221–232, https://doi.org/10.1007/s00382-003-0332-6, 2003.

Hoppel, W. A., Frick, G. M., and Larson, R. E.: Effect of nonprecipitating clouds on the aerosol size distribution in the marine boundary layer, Geophys. Res. Lett., 13(1), 125–128, https://doi.org/10.1029/GL013i002p00125, 1986.

Hudson, J. G. and Noble, S.: CCN and vertical velocity influences on droplet concentrations and supersaturations in clean and polluted stratus clouds, J. Atmos. Sci., 71, 312– 331, https://doi.org/10.1175/JAS-D-13-086.1, 2014.

Igel, A. L., Ekman, A. M. L., Leck, C., Tjernström, M., Savre, J., and Sedlar, J.: The free troposphere as a potential source of Arctic boundary layer aerosol particles, Geophys. Res. Lett., 44, 7053–60, https://doi.org/10.1002/2017GL073808, 2017.

Intrieri, J. M, Shupe, M. D., Uttal, T., and McCarty, B. J.: An annual cycle of Arctic cloud characteristics observed by radar and lidar at SHEBA., J. Geophys. Res. Ocean., 107, 8030, https://doi.org/10.1029/2000JC000423, 2002.

Karl, M., Leck, C., Coz, E., and Heintzenberg, J.: Marine nanogels as a source of atmospheric nanoparticles in the high Arctic, Geophys. Res. Lett., 40, 3738–3743, https://doi.org/10.1002/grl.50661, 2013.

Kay, J. E. and Gettelman, A.: Cloud influence on and response to seasonal arctic sea ice loss, J. Geophys. Res. Atmos., 114, D18204, https://doi.org/10.1029/2009JD011773, 2009.

Kay, J. E., Raeder, K., Gettelman, A., and Anderson, J: The boundary layer response to recent Arctic sea ice loss and implications for high-latitude climate feedbacks, J. Climate, 24, 428–447, https://doi.org/10.1175/2010JCLI3651.1, 2011.

Kecorius, S., Vogl, T., Paasonen, P., Lampilahti, J., Rothenberg, D., Wex, H., Zeppenfeld, S., van Pinxteren, M., Hartmann, M., Henning, S., Gong, X., Welti, A., Kulmala, M., Stratmann, F., Herrmann, H., and Wiedensohler, A.: New particle formation and its effect on cloud condensation nuclei abundance in the summer Arctic: a case study in the Fram Strait and Barents Sea, Atmos. Chem. Phys., 19, 14339–14364, https://doi.org/10.5194/acp-19-14339-2019, 2019.

https://doi.org/10.5194/acp-2020-665
Preprint. Discussion started: 28 July 2020

Atmospheric Chemistry and Physics Discussions

Koike, M., Ukita, J., Ström, J., Tunved, P., Shiobara, M., Vitale, V., A. Lupi, A., Baumgardner, D., Ritter, C., Hermansen, O., Yamada, K., and Pedersen, C. A.: Year-round in situ measurements of Arctic low-level clouds: Microphysical properties and their relationships with aerosols, J. Geophys. Res. Atmos., 124, 1798–1822, https://doi.org/10.1029/2018JD029802, 2019.

Köhler, H.: The nucleus in and the growth of hygroscopic droplets, Trans. Faraday Soc., 32, 1152–1161, https://doi.org/10.1039/TF9363201152, 1936.

Leck, C. and Bigg E. K.: Source and evolution of the marine aerosol—A new perspective, Geophys. Res. Lett., 32, L19803, https://doi.org/10.1029/2005GL023651, 2005a.

Leck, C. and Bigg, E. K.: Biogenic particles in the surface microlayer and overlaying atmosphere in the central Arctic Ocean during summer, Tellus, 57B, 305-316, https://doi.org/10.3402/tellusb.v57i4.16546, 2005b.

Leck, C. and Svensson, E.: Importance of aerosol composition and mixing state for cloud droplet activation over the Arctic pack ice in summer, Atmos. Chem. Phys., 15, 2545–2568, https://doi.org/10.5194/acp-15-2545-2015, 2015.

Leck, C., Bigg, E. K., Covert, D. S., Heintzenberg, J., Maenhaut, W., Nilsson, E. D., and Wiedensohler, A.: Overview of the atmospheric research program during the International Arctic Ocean Expedition 1991 (IAOE-91) and its scientific results, Tellus, 48B, 136-155, https://doi.org/10.3402/tellusb.v48i2.15833, 1996.

Leck, C., Nilsson, E. D., Bigg, E. K., and Bäcklin, L.: Atmospheric program on the Arctic Ocean Expedition 1996 (AOE-96) – An overview of scientific goals, experimental approach, and instrument, J. Geophys. Res., Atmos., 106 (D23), 32,051-32,067, https://doi.org/10.1029/2000JD900461, 2001.

Leck, C., Tjernström, M., Matrai, P., Swietlicki E., and Bigg, E. K.: Can marine micro-organisms influence melting of the Arctic pack ice?, Eos, 85, No3, 25-36, 2004.

Lowe, S. J., Partridge, D. G., Davies, J. F., Wilson, K. R., Topping, D., and Riipinen, I.: Key drivers of cloud response to surface-active organics, Nature Communication, 10:5214, https://doi.org/10.1038/s41467-019-12982-0, 2019.

Lubin, D. and Vogelmann, A. M.: A climatologically significant aerosol longwave indirect effect in the Arctic, Nature, 439(7075), 453–456. https://doi.org/10.1038/nature04449, 2006.

Martin, M., Chang, R. Y.-W., Sierau, B., Sjogren, S., Swietlicki, E., Abbatt, J. P. D., Leck, C., and Lohmann, U.: Cloud condensation nuclei closure study on summer arctic aerosol, Atmos. Chem. Phys., 11, 11335–11350, https://doi.org/10.5194/acp-11-11335-2011, 2011.

Mauritsen, T., Sedlar, J., Tjenström, M., Leck, C., Martin, M., Shupe, M., Sjogren, S., Sierau, B., Persson, P. O. G., Brooks, I. M., and Swietlicki, E.: An Arctic CCN-limited cloud-aerosol regime, Atmos. Chem. Phys., 11, 165–173, https://doi.org/10.5194/acp-11-165-2011, 2011.

Meyers, M. P., Walko, R. L., Harrington, J. Y., and Cotton, W. R.: New RAMS cloud microphysics parameterization. Part II: The two-moment scheme, Atmos. Res., 45(1), 3–39, https://doi.org/10.1016/S0169-8095(97)00018-5, 1997.

Morrison, H. and Grabowski, W.: Modeling supersaturation and subgrid-scale mixing with two-moment bulk warm microphysics, J. Atmos. Sci., 65(3), 792–812, https://doi.org/10.1175/2007JAS2374.1, 2008.

Morrison, H., De Boer, G., Feingold, G., Harrington, J., Shupe, M. D., and Sulia, K.: Resilience of persistent Arctic mixed-phase clouds, Nat. Geosci., 5, 11–17, https://doi.org/10.1038/ngeo1332, 2012.

Ovchinnikov, M., Korolev, A., and Fan, J.: Effects of ice number concentration on dynamics of a shallow mixed-phase stratiform cloud, J. Geophys. Res. Atmos., 116, 1-15, https://doi.org/10.1029/2011JD015888, 2011.

https://doi.org/10.5194/acp-2020-665
Preprint. Discussion started: 28 July 2020

Atmospheric Chemistry and Physics Discussions

Ovchinnikov, M., Ackerman, A. S., Avramov, A., Cheng, A., Fan, J., Fridlind, A. M., Ghan, S., Harrington, J., Hoose, C., Korolev, A., McFarquhar, G. M., Morrison, H., Pauk-ert, M., Savre, J., Shipway, B. J., Shupe, M. D., Solomon, A., and Sulia, K.: Intercomparison of large-eddy simulations of Arctic mixed-phase clouds: Importance of ice size distribution assumptions, J. Adv. Model. Earth Sy., 6, 223–248, https://doi.org/10.1002/2013MS000282, 2014.

Persson, P. O. G., Shupe, M. D., Perovich, D., and Solomon, A.: Linking atmospheric synoptic transport, cloud phase, surface energy fluxes, and sea-ice growth: observations of midwinter SHEBA conditions, Clim. Dyn., 49, 1341–1364, https://doi.org/10.1007/s00382-016-3383-1, 2017.

Petters, M. D. and Kreidenweis, S. M.: A single parameter representation of hygroscopic growth and cloud condensation nucleus activity, Atmos. Chem. Phys., 7, 1961–1971, https://doi.org/10.5194/acp-7-1961-2007, 2007.

Rastak, N., Pajunoja, A., Acosta Navarro, J. C., Ma, J., Song, M., Partridge, D. G., Kirkevåg, A, Leong, Y., Hu, W. W, Taylor, N. F., Lambe, A., Cerully, K., Bougiatioti, A., Liu, P., Krejci, R., Petäjä, T., Percival, C., Davidovits, P., Worsnop, D. R., Ekman, A. M. L., Nenes, A., Martin, S., Jimenez, J. L., Collins, D. R., Topping D.O., Bertram A. K., Zuend, A., Virtanen, A., and Riipinen I.: Microphysical explanation of the RH-dependent water affinity of biogenic organic aerosol and its importance for climate, Geophys. Res. Lett., 44, 5167–5177, https://doi.org/10.1002/2017GL073056, 2017.

Saleeby, S. M. and van den Heever, S. C.: Developments in the CSU-RAMS Aerosol Model: Emissions, Nucleation, Regeneration, Deposition, and Radiation, J. Appl. Meteorol. Climatol., 52, 2601–2622, https://doi.org/10.1175/JAMC-D-12-0312.1, 2013.

Savre, J., Ekman, A. M. L., and Svensson, G.: Technical note: Introduction to MIMICA, a large-eddy simulation solver for cloudy planetary boundary layers, J. Adv. Model. Earth Sy., 6, 1-20, https://doi.org/10.1002/2013MS000292 , 2014.

Sedlar, J. and Shupe, M. D.: Characteristic nature of vertical motions observed in Arctic mixed-phase stratocumulus, Atmos. Chem. Phys., 14, 3461–3478, https://doi.org/10.5194/acp-14-3461-2014, 2014.

Sedlar, J., Shupe, M. D., and Tjernström, M.: On the relationship between thermodynamic structure and cloud top, and its climate significance in the Arctic, J. Climate, 25, 2374–2393, https://doi.org/10.1007/s00382-010-0937-5, 2012.

Seifert, A. and Beheng, K. D.: A double-moment parameterization for simulating autoconversion, accretion and selfcollection., Atmos. Res., 59-60, 265–281, https://doi.org/10.1016/S0169-8095(01)00126-0, 2001.

Seinfeld, J. H. and Pandis, S. N. (2. Ed.): Atmospheric chemistry and physics: From Air pollution to climate change, Wiley, Hoboken, N.J, 2006.

Serreze, M. C. and Barry, R. G.: Processes and impacts of Arctic amplification: A research synthesis, Global and Planetary Change, 77, 85–96, https://doi.org/10.1016/j.gloplacha.2011.03.004, 2011.

Shupe, M. D. and Intrieri, J. M.: Cloud radiative forcing of the Arctic surface: The influence of cloud properties, surface albedo, and solar zenith angle, J. Climate, 17, 616–628, https://doi.org/10.1175/1520-0442(2004)017<0616:CRFOTA>2.0.CO;2, 2004.

Shupe, M. D., Matrosov, S. Y., and Uttal, T.: Arctic mixed-phase cloud properties derived from surface-based sensors at SHEBA, J. Atmos. Sci., 63, 697–711, https://doi.org/10.1175/JAS3659.1, 2006.

Shupe, M. D., Kollias, P., Persson, P. O. G., and McFarquhar, G. M.: Vertical motions in Arctic mixed-phase stratiform clouds, J. Atmos. Sci., 65, 1304–1322, https://doi.org/10.1175/2007JAS2479.1, 2008.

Shupe, M. D., Persson, P. O. G., Brooks, I. M., Tjernström, M., Sedlar, J., Mauritsen, T., Sjogren, S., and Leck, C.: Cloud and boundary layer interactions over the Arctic sea ice in late summer, Atmos. Chem. Phys., 13, 9379–9400, https://doi.org/10.5194/acp-13-9379-2013, 2013.

https://doi.org/10.5194/acp-2020-665
Preprint. Discussion started: 28 July 2020

Atmospheric Chemistry and Physics Discussions

Stevens, B., Moeng, C-H., Ackerman, A. S., Bretherton, C. S., Chlond, A., de Roode, S., Edwards, J., Golaz, J-C., Jlang, H., Khairoutdinov, M., Kirkpatrick, M. P., Lewellen, D. C., Lock, A., Müller, F., Stevens, D. E., Whelen, E., and Zhu, P.: Evaluation of large eddy simulations via observations of nocturnal marine stratocumulus, Monthly Weather Review, 133:1443–1462, https://doi.org/10.1175/MWR2930.1, 2005.

Stevens, R. G., Loewe, K., Dearden, C., Dimitrelos, A., Possner, A., Eirund, G. K., Raatikainen, T., Hill, A. A., Shipway, B. J., Wilkinson, J., Romakkaniemi, S., Tonttila, J., Laaksonen, A., Korhonen, H.m Connolly, P., Lohmann, U., Hoose, C., Ekman, A. M. L., Carslaw, K. S., and Field, P. R.: A model intercomparison of CCN-limited tenuous clouds in the high Arctic, Atmos. Chem. Phys., 18, 11041–11071, https://doi.org/10.5194/acp-18-11041-2018, 2018.

Stjern, C. W., Lund, M. T., Samset, B. H., Myhre, G., Forster, P. M., Andrews, T., Boucher, O., Faluvegi, G., Fläschner, D., Iversen, T., Kasoar, M., Kharin, V., Kirkevåg, A., Lamarque, J., Olivié, D., Richardson, T., Sand, M., Shawki, D., Shindell, D., Smith, C. J., Takemura, T., and Voulgarakis, A.: Arctic amplification response to individual climate drivers, J. Geophys. Res. Atmos., 124, 6698–6717, https://doi.org/10.1029/2018JD029726, 2019.

Tjernström, M.: Is there a diurnal cycle in the summer cloud-capped Arctic boundary layer?, J. Atmos. Sci., 64, 3970–3986, https://doi.org/10.1175/2007JAS2257.1, 2007.

Tjernström, M., Žager, M., Svensson, G., Cassano, J. J, Pfeifer, S., Rinke, A., Wyser, K., Dethloff, K., Jones, C., Semmler, T., and Shaw, M.: Modelling the Arctic boundary layer: An evaluation of six Arcmip regional-scale models using data from the Sheba project, Bound.-Lay. Meteorol., 117, 337-381, https://doi.org/10.1007/s10546-004-7954-z, 2005.

Tjernström, M., Birch, C. E., Brooks, I. M., Shupe, M. D, Persson, P. O. G., Sedlar, J., Mauritsen, T., Leck, C., Paatero, J., Szczodrak, M., and Wheeler, C. R.: Meteorological conditions in the central Arctic summer during the Arctic Summer Cloud Ocean Study (ASCOS), Atmos. Chem. Phys., 12, 6863–6889, https://doi.org/10.5194/acp-12-6863-2012, 2012.

Tjernström, M., Leck, C., Birch, C. E., Bottenheim, J. W., Brooks,B. J., Brooks, I. M., Bäcklin, L., Chang, R. Y.-W., de Leeuw, G.,Di Liberto, L., de la Rosa, S., Granath, E., Graus, M., Hansel,A., Heintzenberg, J., Held, A., Hind, A., Johnston, P., Knulst, J.,Martin, M., Matrai, P. A., Mauritsen, T., Müller, M., Norris, S. J.,Orellana, M. V., Orsini, D. A., Paatero, J., Persson, P. O. G., Gao,Q., Rauschenberg, C., Ristovski, Z., Sedlar, J., Shupe, M. D., Sierau, B., Sirevaag, A., Sjogren, S., Stetzer, O., Swietlicki, E., Szczodrak, M., Vaattovaara, P., Wahlberg, N., Westberg, M., and Wheeler, C. R.: The Arctic Summer Cloud Ocean Study (ASCOS): overview and experimental design, Atmos. Chem. Phys., 14, 2823–2869, https://doi.org/10.5194/acp-14-2823-2014, 2014.

Tjernström, M., Shupe, M. D., Brooks, I. M., Persson, P. O. G., Prytherch, J., Salisbury, D. J., Sedlar, J., Achtert, P., Brooks, B. J., Johnston, P. E., Sotiropoulou, G., and Wolfe, D.: Warm-air advection, air mass transformation and fog causes rapid ice melt, Geophys. Res. Lett., 42, 5594–5602, https://doi.org/10.1002/2015GL064373, 2015.

Walko, R. L., Cotton, W. R., Feingold, G., and Stevens, B.: Efficient computation of vapor and heat diffusion between hydrometeors in a numerical model, Atmos. Res., 53(1-3), 171–183, https://doi.org/10.1016/S0169-8095(99)00044-7, 2000.

Wiedensohler, A., Covert, D. S., Swietlicki, E., Aalto, P. P., Heintzenberg, J., and Leck, C.: Occurrence of an ultrafine particle mode less than 20 nm in diameter in the marine boundary layer during Arctic summer and autumn, Tellus, 48B, 213-222, https://doi.org/10.3402/tellusb.v48i2.15887, 1996.

Willis, M. D., Burkart, J., Thomas, J. L., Köllner, F., Schneider, J. Bozem, H., Hoor, P. M., Aliabadi, A. A., Schulz, H., Herber, A. B., Leaitch, W. R., and Abbatt, J. P. D.: Growth of nucleation mode particles in the summertime Arctic: a case study, 16, 7663-7679, Atmos. Chem. Phys., https://doi.org/10.5194/acp-16-7663-2016, 2016.

Yang, F., McGraw, R., Luke, E. P., Zhang, D., Kollias, P., and Vogelmann, A. M.: A new approach to estimate supersaturation fluctuations in stratocumulus cloud using ground-based remote-sensing measurements, Atmos. Meas. Tech., 12, 5817–5828, https://doi.org/10.5194/amt-12-5817-2019, 2019.